01 Mar 2023

Error Analysis of a Fully Discrete Projection Method for Magnetohydrodynamic System

Qianqian Ding

Xiaoming He
Missouri University of Science and Technology, hex@mst.edu

Xiaonian Long

Shipeng Mao

Recommended Citation
Q. Ding et al., "Error Analysis of a Fully Discrete Projection Method for Magnetohydrodynamic System," *Numerical Methods for Partial Differential Equations*, vol. 39, no. 2, pp. 1449 - 1477, Wiley, Mar 2023.
The definitive version is available at https://doi.org/10.1002/num.22941

Received: 31 August 2020 | Revised: 17 December 2020 | Accepted: 28 September 2022 | Published on: 5 November 2022

DOI: 10.1002/num.22941

RESEARCH ARTICLE

WILEY

Error analysis of a fully discrete projection method for magnetohydrodynamic system

Qianqian Ding[1] | **Xiaoming He**[2] | **Xiaonian Long**[3] | **Shipeng Mao**[4]

[1]School of Mathematics, Shandong University, Jinan, China
[2]Department of Mathematics and Statistics, Missouri University of Science and Technology, Rolla, Missouri, USA
[3]College of Mathematics and Information Science, Henan University of Economics and Law, Zhengzhou, China
[4]LSEC and ICMSEC, Academy of Mathematics and Systems Science, Chinese Academy of Sciences, School of Mathematical Science, University of Chinese Academy of Sciences, Beijing, China

Correspondence
Shipeng Mao, LSEC and ICMSEC, Academy of Mathematics and Systems Science, Chinese Academy of Sciences, School of Mathematical Science, University of Chinese Academy of Sciences, Beijing 100190, China.
Email: maosp@lsec.cc.ac.cn

Funding information
National Natural Science Foundation of China, Grant/Award Numbers: 11871467, 12271514, 12201353; Natural Science Foundation of Shandong Province, Grant/Award Number: ZR2021QA054.

Abstract

In this paper, we develop and analyze a finite element projection method for magnetohydrodynamics equations in Lipschitz domain. A fully discrete scheme based on Euler semi-implicit method is proposed, in which continuous elements are used to approximate the Navier–Stokes equations and $\boldsymbol{H}(\boldsymbol{curl})$ conforming Nédélec edge elements are used to approximate the magnetic equation. One key point of the projection method is to be compatible with two different spaces for calculating velocity, which leads one to obtain the pressure by solving a Poisson equation. The results show that the proposed projection scheme meets a discrete energy stability. In addition, with the help of a proper regularity hypothesis for the exact solution, this paper provides a rigorous optimal error analysis of velocity, pressure and magnetic induction. Finally, several numerical examples are performed to demonstrate both accuracy and efficiency of our proposed scheme.

KEYWORDS

error analysis, finite element method, magnetohydrodynamics, Nédélec edge element, projection methods

1 | INTRODUCTION

In recent years, the significance of magnetohydrodynamics (MHD) has increased with respect to scientific and engineering problems. Many interesting MHD flows involve a viscous, incompressible, conductive fluid that interacts with electromagnetic inductions, compare [1–4] and references therein. Therefore, a significant amount of research works have been carried out for numerical methods for the MHD equations, see, for example [2, 5–20] and the references therein.

Among all the developed methods for the MHD equations, here we are particularly interested in the projection methods, whose original versions were proposed by Chorin and Temam in [21, 22], because of its efficiency and simplicity features [23–25]. The most attractive feature of projection methods is that, at each time step, one only needs to solve a sequence of decoupled equations for velocity and pressure. Rannacher in [26] derived improved optimal first order error estimates for the original projection scheme introduced by Chorin and Temam (see also [27] or [28]). Some rigorous error analysis of projection methods in temporal discretization were also carried out for incompressible Navier–Stokes equations [29–35].

However, it is not an easy job to prove the error analysis of fully discrete scheme based on projection methods, because it must be compatible with two different spaces when calculating velocity. Compared with the numerous articles on the temporal discretization for projection methods, there are only a relatively small number of papers on the analysis for the finite element projection methods with a fully discrete scheme. For example, a fully discrete velocity-correction scheme for Stokes problem was proposed in [36]. A fractional-step projection method for calculating incompressible Navier–Stokes flows by using finite element method was developed in [37], and it laid a foundation for our research in this paper. For the time-dependent incompressible MHD problems, the authors in [38] developed several efficient numerical schemes and proved the error estimates for the semi time-discrete case. Recently, a linear, unconditionally stable projection methods and the error estimates for the time-discrete MHD system had been proved in [39]. A fully discrete projection methods with unconditional energy stable scheme for MHD problem had been developed in [40], in which the magnetic induction was approximated by Lagrange element and the numerical experiments were carried out in a two-dimensional convex domain. We remark that all these articles assume that the domain is either convex or has a $C^{1,1}$ boundary and the magnetic induction $\boldsymbol{B} \in \boldsymbol{H}^1(\Omega)$, so that the magnetic induction can be discretized by continuous Lagrange finite element method by adding $\operatorname{div}\boldsymbol{B}$ to the Maxwell equation. However, it is well known that continuous Lagrange finite element discretization may not converge to the correct magnetic induction for non-convex domain or Lipschitz polyhedral domain (see, e.g., [41–44]), which is frequently encountered in practical engineering computations. A possible way to overcome these difficulties was proposed in [45] by virtue of Nédélec finite elements for the magnetic induction $\boldsymbol{B}$. On the other hand, Nédélec finite elements approximation to the magnetic induction in MHD system seems to be a natural choice since it can treat the boundary conditions of magnetic induction $\boldsymbol{B}$ easier than continuous finite element discretization. For the unsteady system, a semi-implicit finite element scheme based on Nédélec edge elements for the incompressible MHD equations was studied in [46], in which the energy preservation is proved and an optimal error estimate under low regularity assumption is derived. The study of Nédélec finite elements approximation to the magnetic induction in MHD system is attractive and it has been employed in [16, 47–49]. We also mention the recent papers [6, 19], where different formulations were proposed to maintain the divergence free magnetic solutions in the numerical schemes.

In this paper, we will propose and study an effective projection numerical method for three dimensional MHD flows by using continuous elements to approximate the Navier–Stokes equations and Nédélec edge elements to approximate the magnetic equation. The proposed scheme can be used for the domain may be a non-convex polyhedra and the magnetic induction $\boldsymbol{B}$ has regularity lower than $\boldsymbol{H}^1(\Omega)$ since the Nédélec edge element discretization can capture the physics solutions, which is a natural choice to solve the Maxwell equations in the field of scientific computing. One key requirement of projection method is that it must be compatible with two different spaces for calculating velocity, which makes the error estimation quite technical. What is more, the low magnetic induction regularity and loss of divergence control will bring new difficulties to theoretical analysis and some special techniques need to be developed. As a result, a rigorous optimal error analysis of velocity, pressure, and

magnetic induction is presented in this article. In addition, we carry out numerical experiments on the projection scheme for three dimensional MHD flows to verify to illustrate its stability and accuracy, which agree well with the theoretical results.

The outline of this work is organized as follows. In Section 2, we describe the MHD model, the notations and the basic facts to be used throughout the paper. We propose a proper weak solution for the MHD model and provide the energy estimates. In Section 3, we design a fully discrete scheme based on projection method. The unconditional energy stability of the fully discrete scheme is shown. In Section 4, we derive the error estimates for velocity, pressure, and magnetic induction. In Section 5, some numerical experiments are carried out to test the behavior of the numerical solution. Finally, we close the paper with some concluding remarks in Section 6.

2 | THE MHD MODEL

Let Ω be a bounded domain with Lipschitz boundary $\partial\Omega$ in $\mathbb{R}^3$, we consider the following incompressible MHD equations:

$$\begin{cases} \boldsymbol{u}_t - \nu\Delta\boldsymbol{u} + (\boldsymbol{u}\cdot\nabla)\boldsymbol{u} + \nabla p + \kappa\boldsymbol{B}\times\operatorname{curl}\boldsymbol{B} = \boldsymbol{f} \quad \text{in } Q_T, & (2.1)\\ \boldsymbol{B}_t + R_m^{-1}\operatorname{curl}\boldsymbol{B} - \operatorname{curl}(\boldsymbol{u}\times\boldsymbol{B}) = 0 \quad \text{in } Q_T, & (2.2)\\ \operatorname{div}\boldsymbol{u} = 0 \quad \text{in } Q_T, & (2.3)\\ \operatorname{div}\boldsymbol{B} = 0 \quad \text{in } Q_T, & (2.4) \end{cases}$$

where $Q_T = \Omega\times(0,T)$, $T>0$ is a given finite final time, $\boldsymbol{u}$ denotes the velocity field, p the pressure, $\boldsymbol{B}$ the magnetic induction, ν the kinematic viscosity, κ the coupling number, R_m the magnetic Reynolds number, and $\boldsymbol{f}$ the given source term. The system (2.1)–(2.4) is considered in conjunction with the following boundary conditions and initial values,

$$\begin{aligned} &\boldsymbol{u} = 0, \qquad \boldsymbol{B}\times\boldsymbol{n} = 0 \qquad \text{on } S_T,\\ &\boldsymbol{u}(t_0) = \boldsymbol{u}^0, \qquad \boldsymbol{B}(t_0) = \boldsymbol{B}^0 \qquad \text{in } \Omega, \end{aligned} \tag{2.5}$$

where $S_T = \partial\Omega\times(0,T)$, $\boldsymbol{n}$ is the outer unit normal of $\partial\Omega$ and the initial magnetic induction $\boldsymbol{B}^0$ satisfies div $\boldsymbol{B}^0 = 0$. Our results are also valid for another frequently used set of boundary conditions of the magnetic induction $\boldsymbol{B}$:

$$\boldsymbol{B}\cdot\boldsymbol{n} = 0, \qquad \boldsymbol{n}\times\operatorname{curl}\mathrm{B} = 0 \qquad \text{on } S_T.$$

But we shall mainly consider the boundary conditions (2.5) in this paper.

For mathematical setting of the problem (2.1)–(2.5), we first introduce some notations that will be used throughout the paper. For all $m\in\mathbb{N}^+$, $1\le p\le\infty$, let $W^{m,p}(\Omega)$ denote the standard Sobolev space and it is written as $H^m(\Omega)$ when $p=2$. The norm in $W^{m,p}(\Omega)$ is defined by $\|\cdot\|_{m,p}$ such that

$$\begin{aligned} &\|v\|_{m,p} = \left(\sum_{|\alpha|\le m}\|D^\alpha v\|_{0,p}^p\right)^{1/p} \quad \text{with } \|v\|_{0,p} = \left(\int_\Omega |v|^p\,dx\right)^{1/p}, 1\le p<\infty,\\ &\|v\|_{m,\infty} = \max_{|\alpha|\le m}\|D^\alpha v\|_{0,\infty} \quad \text{with } \|v\|_{0,\infty} = \operatorname*{ess\,sup}_{\mathrm{x}\in\Omega}|\mathrm{v}(\mathrm{x})|, \end{aligned}$$

where

$$D^\alpha = \frac{\partial^{|\alpha|}}{\partial x_1^{\alpha_1}\partial x_2^{\alpha_2}\partial x_3^{\alpha_3}},$$

for the multi-index $\alpha = (\alpha_1, \alpha_2, \alpha_3)$ and $|\alpha| = \alpha_1 + \alpha_2 + \alpha_3$, with $\alpha_1, \alpha_2, \alpha_3 \geq 0$. For the function spaces $L^p(0, T; X)$, $1 \leq p \leq \infty$, the norms are denoted as

$$\|v\|_{L^p(0,T;X)} = \left(\int_0^T \|v(t)\|_X^p \, dt\right)^{1/p} \qquad \text{for } 1 \leq p < +\infty,$$
$$\|v\|_{L^\infty(0,T;X)} = \text{ess} \sup_{0 \leq t \leq T} \|v(t)\|_X,$$

where X is a real Banach space with the norm $\|\cdot\|_X$. The inner product will be denoted by $(\cdot, \cdot)$, that is $(\phi, \psi) = \int_\Omega \phi\psi \, dx$ and the norm in $L^2(\Omega)$ defined by $\|\cdot\|_0$. Vector-valued quantities will be denoted in boldface notations, such as $\boldsymbol{u} = (u_1, u_2, u_3)$ and $\boldsymbol{L}^2(\Omega) = (L^2(\Omega))^3$. We use C and c, with or without subscripts, bars, tildes or hats, to denote generic positive constants independent of the discretization parameters, which may take different values at different places.

We introduce the following classical Sobolev spaces:

$$\boldsymbol{X} = \boldsymbol{H}_0^1(\Omega), \qquad \boldsymbol{X}_0 = \{\boldsymbol{u} \in \boldsymbol{X}, \operatorname{div} \boldsymbol{u} = 0\}, \qquad M = L_0^2(\Omega),$$
$$\boldsymbol{W} = \left\{\boldsymbol{C} \in \boldsymbol{L}^2(\Omega), \operatorname{curl} \boldsymbol{C} \in \boldsymbol{L}^2(\Omega)\right\}, \qquad \boldsymbol{W}_0 = \{\boldsymbol{C} \in \boldsymbol{W}, \boldsymbol{C} \times \boldsymbol{n}\big|_{\partial\Omega} = 0\}.$$

Here and in what follows, we define the norm

$$\|\boldsymbol{C}\|_{\boldsymbol{W}} = \|\boldsymbol{C}\|_{\boldsymbol{H}(\text{curl};\Omega)} = \left(\|\boldsymbol{C}\|_0^2 + \|\operatorname{curl} \boldsymbol{C}\|_0^2\right)^{1/2} \qquad \forall \boldsymbol{C} \in \boldsymbol{W}.$$

It is well known that the following Poincaré type and embedding inequalities are valid in bounded polyhedral domains (see chapter 3 of [50] for more details),

$$\|\boldsymbol{v}\|_{0,m} \leq c_1 \|\nabla \boldsymbol{v}\|_0, \qquad m \in [1, 6] \qquad \forall \boldsymbol{v} \in \boldsymbol{X}, \tag{2.6}$$
$$\|\operatorname{curl} \boldsymbol{v}\|_{0,3} \leq c_2 \|\operatorname{curl} \boldsymbol{v}\|_{s,2} \qquad \forall \boldsymbol{v} \in \boldsymbol{W} \qquad \forall s > 1/2, \tag{2.7}$$
$$\|\boldsymbol{v}\|_{0,\infty} \leq c_3 \|\boldsymbol{v}\|_{1+s,2} \qquad \forall s > 1/2, \tag{2.8}$$
$$\|\boldsymbol{v}\|_{1,3} \leq c_4 \|\boldsymbol{v}\|_{1+s,2} \qquad \forall s > 1/2. \tag{2.9}$$

We denote

$$c(\boldsymbol{w}, \boldsymbol{u}, \boldsymbol{v}) = \frac{1}{2}[((\boldsymbol{w} \cdot \nabla)\boldsymbol{u}, \boldsymbol{v}) - ((\boldsymbol{w} \cdot \nabla)\boldsymbol{v}, \boldsymbol{u})] \qquad \forall \boldsymbol{w}, \boldsymbol{u}, \boldsymbol{v} \in \boldsymbol{X}.$$

It can be checked that the following identity holds by the divergence theorem

$$c(\boldsymbol{w}, \boldsymbol{u}, \boldsymbol{v}) = ((\boldsymbol{w} \cdot \nabla)\boldsymbol{u}, \boldsymbol{v}) + \frac{1}{2}((\operatorname{div} \boldsymbol{w})\boldsymbol{u}, \boldsymbol{v}).$$

We now introduce the operators which will be used below, $\mathscr{B} : \boldsymbol{X} \to M$, $\mathscr{B}^T : M \to \boldsymbol{X}'$, for any $\boldsymbol{v} \in \boldsymbol{X}$, $q \in M$ such that $(\mathscr{B}\boldsymbol{v}, q) = \left(\boldsymbol{v}, \mathscr{B}^T q\right) = -(\operatorname{div} \boldsymbol{v}, q)$.

2.1 | Weak solution of the MHD model

We describe the definition of weak solution to problem (2.1)–(2.5) as follows [16].

Definition 1 Let $\boldsymbol{u}^0 \in \boldsymbol{X}_0$ and $\boldsymbol{B}^0 \in \boldsymbol{W}_0$. The triple $(\boldsymbol{u}, p, \boldsymbol{B})$ is called a weak solution of the system (2.1)–(2.5), if it satisfies $\boldsymbol{u} \in L^\infty\left(0, T; \boldsymbol{L}^2(\Omega)\right) \cap L^2(0, T; \boldsymbol{X}_0)$, $p \in L^\infty(0, T; M)$ and $\boldsymbol{B} \in L^\infty\left(0, T; \boldsymbol{L}^2(\Omega)\right) \cap L^2(0, T; \boldsymbol{W}_0)$ such that

$$\begin{cases} (\boldsymbol{u}_t, \boldsymbol{v}) + \nu(\nabla \boldsymbol{u}, \nabla \boldsymbol{v}) + c(\boldsymbol{u}, \boldsymbol{u}, \boldsymbol{v}) + \left(\mathscr{B}^T p, \boldsymbol{v}\right) + \kappa(\boldsymbol{B} \times \operatorname{curl} \boldsymbol{B}, \boldsymbol{v}) - (\mathscr{B}\boldsymbol{u}, q) = (\boldsymbol{f}, \boldsymbol{v}), & (2.10) \\ (\boldsymbol{B}_t, \boldsymbol{C}) + R_m^{-1}(\operatorname{curl} \boldsymbol{B}, \operatorname{curl} \boldsymbol{C}) - (\boldsymbol{u} \times \boldsymbol{B}, \operatorname{curl} \boldsymbol{C}) = 0, & (2.11) \end{cases}$$

for any $(\boldsymbol{v}, q, \boldsymbol{C}) \in (\boldsymbol{X}_0 \times M \times \boldsymbol{W}_0)$ and almost all $t \in (0, T]$.

The existence of the solution to (2.10)–(2.11) was proved in [2, 16]. In this paper, we mainly analyze the error estimate by using finite element projection methods. The system (2.10)–(2.11) enjoys the following energy law and the main feature of the MHD system is that it is a dissipative system.

Theorem 1 *For any* $\boldsymbol{u}(t)$, $\boldsymbol{B}(t)$ *and* $p(t)$ *that satisfy* (2.10)–(2.11), *the following energy stability result holds*

$$\int_0^t \left(\nu\|\nabla\boldsymbol{u}(t)\|_0^2 + R_m^{-1}\kappa\|\mathrm{curl}\boldsymbol{B}(t)\|_0^2\right) dt + \frac{1}{2}\|\boldsymbol{u}(t)\|_0^2 + \frac{\kappa}{2}\|\boldsymbol{B}(t)\|_0^2 = \frac{1}{2}\|\boldsymbol{u}(0)\|_0^2 + \frac{\kappa}{2}\|\boldsymbol{B}(0)\|_0^2 + \int_0^t (\boldsymbol{f},\boldsymbol{u})\,dt.$$

Proof. By choosing $\boldsymbol{v} = \boldsymbol{u}$, $q = p$ in (2.10), $\boldsymbol{C} = \kappa\boldsymbol{B}$ in (2.11) and adding up the two equations, we can deduce that

$$\frac{1}{2}\frac{\partial}{\partial t}\|\boldsymbol{u}\|_0^2 + \frac{\kappa}{2}\frac{\partial}{\partial t}\|\boldsymbol{B}\|_0^2 + \nu\|\nabla\boldsymbol{u}\|_0^2 + R_m^{-1}\kappa\|\mathrm{curl}\boldsymbol{B}\|_0^2 = (\boldsymbol{f},\boldsymbol{u}). \tag{2.12}$$

Integrating (2.12) from 0 to t, Theorem 1 is proved. ■

Remark 1 Under the external force $(\boldsymbol{f}, \boldsymbol{u})$, the total energy contains the fluid kinetic energy $\frac{1}{2}\|\boldsymbol{u}(t)\|_0^2$ and the magnetic energy $\frac{\kappa}{2}\|\boldsymbol{B}(t)\|_0^2$, while the dissipation of energy includes the friction losses $\nu\|\nabla\boldsymbol{u}(t)\|_0^2$ and the Ohmic losses $R_m^{-1}\kappa\|\mathrm{curl}\boldsymbol{B}(t)\|_0^2$.

3 | A FULLY DISCRETE FINITE ELEMENT PROJECTION METHOD FOR MHD SYSTEM

As we can see from the contents of the previous section, MHD is a system with nonlinear full coupling of velocity, pressure and magnetic field variables. Especially, the velocity and the pressure are coupled by the incompressible constraint, which brings great difficulties to the actual numerical calculation. In this section, we introduce a fully discrete projection finite element method for problem (2.10)–(2.11) based on Euler semi-implicit scheme. This scheme enables us to solve only a sequence of decoupled linear equations at each time step.

Let Ω be a Lipschitz polyhedral domain and let $\mathcal{T}_h$ be a regular, quasi-uniform triangulation of Ω, where h is the maximal diameter of the element in the mesh [51, 52]. Let $P_k(K)$ be the space of polynomials of total degree at most $k \geq 0$ on K and $\widetilde{P}_k(K)$ the space of homogeneous polynomials k on K. Let $\boldsymbol{X}_h \subset \boldsymbol{X}$ and $M_h \subset M$ be a pair of mixed finite element spaces based on the triangulation $\mathcal{T}_h$. We assume $\boldsymbol{X}_h$ is the k order vectorial Lagrange finite element space and M_h is the $k-1$ order scalar Lagrange finite element space.

The space $\mathcal{D}_k(K)$ denotes the polynomials $\boldsymbol{q}$ in $\widetilde{\boldsymbol{P}}_k(K)$ that satisfy $\boldsymbol{q}(x) \cdot \boldsymbol{x} = 0$ on K. For $1 \leq k$, we define the space

$$\mathcal{N}_k(K) = \boldsymbol{P}_{k-1}(K) \oplus \mathcal{D}_k(K).$$

To approximate the magnetic induction, we use Nédélec $\boldsymbol{H}$(curl)-conforming finite element space (see [50, 53]), which is defined by

$$\boldsymbol{W}_h = \{\boldsymbol{C} \in \boldsymbol{W}_0, \boldsymbol{C}|_K \in \mathcal{N}_k(K) \qquad \forall K \in \mathcal{T}_h\}.$$

Note that the above definition is the first family $\boldsymbol{H}$(curl)-conforming discrete space. We can also employ the second family finite element spaces with $\mathcal{N}_k(K)$ chosen by $\boldsymbol{P}_k(K)$. They are natural choice to discrete the Maxwell equations.

Setting $S_h = \left\{C \in H^1(\Omega) \cap L_0^2(\Omega), C \in P_k(K), \forall K \in \mathcal{T}_h\right\}$, we introduce the discretely solenoidal function space $\boldsymbol{W}_{0h}$

$$\boldsymbol{W}_{0h} = \{\boldsymbol{B}_h \in \boldsymbol{W}_h, (\boldsymbol{B}_h \nabla s_h) = 0 \qquad \forall s_h \in S_h\}.$$

Furthermore, the space $\boldsymbol{W}_{0h}$ is known to satisfy the following discrete Poincaré–Friedrichs inequality:

$$\|\boldsymbol{C}_h\|_0 \le c_* \|\mathrm{curl}\, \boldsymbol{C}_h\|_0 \qquad \text{for } \boldsymbol{C}_h \in \boldsymbol{W}_{0h}, \tag{3.1}$$

where $c_* > 0$ independent of the mesh-size h (see theorem 4.7 of [54] or [45]).

Let $\boldsymbol{Z}_h$ be finite dimensional subspace of $\boldsymbol{L}^2(\Omega)$ and satisfy $\boldsymbol{X}_h \subset \boldsymbol{Z}_h$. Furthermore, we assume that $\boldsymbol{Z}_h$ and M_h are compatible in the sense that either $\boldsymbol{Z}_h$ is conformal in

$$\boldsymbol{H}_0(\mathrm{div}\,\Omega) = \{\boldsymbol{v} \in \boldsymbol{L}^2(\Omega), \qquad \mathrm{div}\,\boldsymbol{v} \in L^2(\Omega), \qquad \boldsymbol{v} \cdot \boldsymbol{n}|_{\partial\Omega} = 0\}$$

or M_h is conformal in $H^1(\Omega)$.

We recall the following inverse estimate from theorem 3.2.6 of [55]. On a quasi-uniform mesh there holds

$$\|\boldsymbol{v}_h\|_{m,q} \le C_{inv} h^{\iota - m + 3(1/q - 1/p)} \|\boldsymbol{v}_h\|_{\iota,p} \qquad \forall \boldsymbol{v}_h \in \boldsymbol{X}_h, \tag{3.2}$$

where $C_{inv} > 0$ is a generic constant independent of the mesh-size h, ι and m are two real numbers with $0 \le \iota \le m \le 1$, p and q are two integers with $1 \le p \le q \le \infty$.

We assume the finite element pair $\boldsymbol{X}_h$ and M_h is inf-sup compatible. That is to say, the following discrete inf-sup condition (see, e.g., chapter 2 of [51, 52, 56]) holds.

Lemma 1 *For any $q_h \in M_h$, there exists $\boldsymbol{v}_h \in \boldsymbol{X}_h$ satisfies the discrete inf-sup condition*

$$\inf_{0 \ne q_h \in M_h} \sup_{\boldsymbol{0} \ne \boldsymbol{v}_h \in \boldsymbol{X}_h} \frac{(\mathrm{div}\,\boldsymbol{v}_h, q_h)}{\|\boldsymbol{v}_h\|_{1,2} \|q_h\|_0} \ge \beta_1, \tag{3.3}$$

where β_1 is a generic positive constant depending on the domain Ω.

We introduce the linear operator $\mathscr{B}_h : \boldsymbol{X}_h \to M_h$ and its transpose $\mathscr{B}_h^T : M_h \to \boldsymbol{X}_h$. For any $\boldsymbol{v}_h \in \boldsymbol{X}_h$, $q_h \in M_h$, one can obtain $(\mathscr{B}_h \boldsymbol{v}_h, q_h) = \left(\boldsymbol{v}_h, \mathscr{B}_h^T q_h\right)$. We assume $\mathscr{B}_h$ is surjective, which means that $\mathscr{B}_h$ satisfies the inf-sup condition (3.3). In order to analyze the spatial error of the projection methods, a discrete divergence operator $\mathscr{C}_h$ needs to be introduced, where $\mathscr{C}_h : \boldsymbol{Z}_h \to M_h$ and its transpose $\mathscr{C}_h^T : M_h \to \boldsymbol{Z}_h$. For any $\boldsymbol{v}_{1h} \in \boldsymbol{Z}_h$, $q_h \in M_h$, either $(\mathscr{C}_h \boldsymbol{v}_{1h}, q_h) = -(\mathrm{div}\,\boldsymbol{v}_{1h}, q_h)$ if $\boldsymbol{Z}_h \subset \boldsymbol{H}_0(\mathrm{div};\Omega)$ or $(\mathscr{C}_h \boldsymbol{v}_{1h}, q_h) = (\boldsymbol{v}_{1h}, \nabla q_h)$ if $M_h \subset H^1(\Omega)$. In addition, we define the continuous injection $\mathscr{I}_h : \boldsymbol{X}_h \to \boldsymbol{Z}_h$, and $\mathscr{I}_h^T$ is the transpose of $\mathscr{I}_h$, namely, the $\boldsymbol{L}^2$-orthogonal projection onto $\boldsymbol{X}_h$.

The relationship between $\mathscr{B}_h$ and $\mathscr{C}_h$ can be described as follows.

Lemma 2 *The operator $\mathscr{C}_h$ is an extension of $\mathscr{B}_h$ and $\mathscr{I}_h^T \mathscr{C}_h^T = \mathscr{B}_h^T$, namely, we have the following commutative diagram (see [37] for more details),*

$$\begin{tikzcd}
& \boldsymbol{M}_h \arrow[dl, shift right, "\mathscr{C}_h^T"'] \arrow[dr, shift left, "\mathscr{B}_h^T"] & \\
\boldsymbol{Z}_h \arrow[ur, shift right, "\mathscr{C}_h"'] \arrow[rr, shift right, "\mathscr{I}_h^T"'] & & \boldsymbol{X}_h \arrow[ul, shift left, "\mathscr{B}_h"] \arrow[ll, shift right, "\mathscr{I}_h"']
\end{tikzcd}$$

Remark 2 If $\boldsymbol{X}_h = \boldsymbol{Z}_h$, the operators $\mathscr{B}_h$ and $\mathscr{C}_h$ involved in Lemma 2 are identical, namely, $\mathscr{B}_h = \mathscr{C}_h$. We know that $\mathscr{B}_h$ is assumed to be surjective, so $\mathscr{C}_h$ is also surjective.

In the following analysis, we consider the fully discrete finite element method based on Euler semi-implicit scheme. Let $N > 0$ be a fixed integer number and $\Delta t = T/N$ be the time-step size. Then $t_n = n\Delta t$, $n = 1, 2, \ldots, N$ denote the discrete time levels. For convenience, we introduce the notation $d_t \boldsymbol{w}^n = (\boldsymbol{w}^n - \boldsymbol{w}^{n-1})/\Delta t$ with $\boldsymbol{w}^n = \boldsymbol{w}(t_n)$.

With the above notations, we now propose the fully discrete variational scheme of (2.10)–(2.11) via the following two-steps.

Step 1 Given $\widetilde{\boldsymbol{u}}_h^{n-1}$, p_h^{n-1} and $\boldsymbol{B}_h^{n-1}$, for any $(\boldsymbol{v}_h, \boldsymbol{C}_h) \in (\boldsymbol{X}_h \times \boldsymbol{W}_h)$, find $\widetilde{\boldsymbol{u}}_h^n \in \boldsymbol{X}_h$ and $\boldsymbol{B}_h^n \in \boldsymbol{W}_h$ such that

$$\begin{cases} \left(\frac{\widetilde{\boldsymbol{u}}_h^n - \mathscr{I}_h^T \boldsymbol{u}_h^{n-1}}{\Delta t}, \boldsymbol{v}_h\right) + c\left(\widetilde{\boldsymbol{u}}_h^{n-1}, \widetilde{\boldsymbol{u}}_h^n, \boldsymbol{v}_h\right) + \nu\left(\nabla \widetilde{\boldsymbol{u}}_h^n, \nabla \boldsymbol{v}_h\right) + \left(\mathscr{B}_h^T p_h^{n-1}, \boldsymbol{v}_h\right) \\ \quad +\kappa\left(\boldsymbol{B}_h^{n-1} \times \operatorname{curl} \boldsymbol{B}_h^n, \boldsymbol{v}_h\right) = \left(\boldsymbol{f}^n, \boldsymbol{v}_h\right), & (3.4) \\ \left(d_t \boldsymbol{B}_h^n, \boldsymbol{C}_h\right) + \frac{1}{R_m}\left(\operatorname{curl} \boldsymbol{B}_h^n, \operatorname{curl} \boldsymbol{C}_h\right) - \left(\widetilde{\boldsymbol{u}}_h^n \times \boldsymbol{B}_h^{n-1}, \operatorname{curl} \boldsymbol{C}_h\right) = 0. & (3.5) \end{cases}$$

Step 2 Given $\widetilde{\boldsymbol{u}}_h^n$, p_h^{n-1}, for any $(\boldsymbol{v}_{1h}, q_h) \in (\boldsymbol{Z}_h \times M_h)$, find $\boldsymbol{u}_h^n \in \boldsymbol{Z}_h$ and $p_h^n \in M_h$ such that

$$\begin{cases} \left(\frac{\boldsymbol{u}_h^n - \mathscr{I}_h \widetilde{\boldsymbol{u}}_h^n}{\Delta t}, \boldsymbol{v}_{1h}\right) + \left(\mathscr{C}_h^T\left(p_h^n - p_h^{n-1}\right), \boldsymbol{v}_{1h}\right) = 0, & (3.6) \\ \left(\mathscr{C}_h \boldsymbol{u}_h^n, q_h\right) = 0. & (3.7) \end{cases}$$

With initial values satisfy $\widetilde{\boldsymbol{u}}_h^0 = \boldsymbol{u}_h^0$ to approximate $\boldsymbol{u}(t_0)$, $\boldsymbol{B}_h^0$ to approximate $\boldsymbol{B}(t_0)$, and p_h^0 to approximate $p(t = 0)$ such that satisfy (4.5).

Remark 3 The original Chorin-Temam projection method does not contain $\mathscr{B}_h^T p_h^{n-1}$ in (3.4) and only contains the unknown p_h^n in (3.6) (see, e.g., [26, 57, 58]). Applying div operator on both sides of (3.6) simultaneously, the system (3.6)–(3.7) is equivalent to solve a discrete Poisson problem for the pressure. When the pressure is solved, by virtue of $\boldsymbol{u}_h^n = \mathscr{I}_h \widetilde{\boldsymbol{u}}_h^n + \Delta t \mathscr{C}_h^T\left(p_h^n - p_h^{n-1}\right)$, then we arrive at $\boldsymbol{u}_h^n$. Note that the scheme (3.4)–(3.7) is just a projection algorithm framework and may use various forms chosen by the users. Specifically, we will show how this method can be implemented in the particular situation $\boldsymbol{Z}_h = \boldsymbol{X}_h + \nabla M_h$ in Section 5.

Remark 4 When Ω is a non-convex polyhedron or non $C^{1,1}$ smooth boundary, the difficulty comes from the fact that the magnetic induction is in general not in $\boldsymbol{H}^1(\Omega)$ (see remark 3.3.1 of [2] for an explanation). The approximation of the magnetic induction with classical nodal element may miss singularities in the physical solution, due to re-entrant corners. This is the reason why we choose Nédélec edge elements to approximate the magnetic induction in (3.5) (cf., for instance, [2, 42, 44] etc).

Remark 5 The scheme (3.5) satisfies a weakly divergence free property. That is to say, by choosing $\boldsymbol{C}_h = \nabla s_h$ in (3.5), where $s_h \in S_h$, thanks to curl $\nabla = 0$, we can obtain $\left(d_t \boldsymbol{B}_h^n, \nabla s_h\right) = 0$, namely, $\left(\left(\boldsymbol{B}_h^n - \boldsymbol{B}_h^{n-1}\right)/\Delta t, \nabla s_h\right) = 0$. Due to $\left(\boldsymbol{B}_h^0, \nabla s_h\right) = 0$, it is easy to deduce $\left(\boldsymbol{B}_h^n, \nabla s_h\right) = 0$, for all $n \geq 1$.

A fully discrete energy law of the solution to problem (3.4)–(3.7) is given, which plays an important role in proving the subsequent error analysis.

Lemma 3 *Let* $\left(\boldsymbol{u}_h^n, \widetilde{\boldsymbol{u}}_h^n, p_h^n, \boldsymbol{B}_h^n\right)$ *be the solution of* (3.4)–(3.7), *then the following stability result is obtained*

$$\begin{aligned}
&\|\boldsymbol{u}_h^m\|_0^2 + 2(\Delta t)^2\left\|\mathscr{C}_h^T p_h^m\right\|_0^2 + \kappa\|\boldsymbol{B}_h^m\|_0^2 + \sum_{n=1}^m\left(\left\|\widetilde{\boldsymbol{u}}_h^n - \mathscr{I}_h^T\boldsymbol{u}_h^{n-1}\right\|_0^2\right.\\
&\left.+\kappa\left\|\boldsymbol{B}_h^n - \boldsymbol{B}_h^{n-1}\right\|_0^2 + 2\Delta t\nu\|\nabla\widetilde{\boldsymbol{u}}_h^n\|_0^2 + 2\Delta t\kappa R_m^{-1}\|\operatorname{curl}\boldsymbol{B}_h^n\|_0^2\right)\\
&= \left\|\mathscr{I}_h^T\boldsymbol{u}_h^0\right\|_0^2 + 2(\Delta t)^2\left\|\mathscr{C}_h^T p_h^0\right\|_0^2 + \kappa\left\|\boldsymbol{B}_h^0\right\|_0^2 + 2\Delta t\sum_{n=1}^m\left(\boldsymbol{f}^n, \widetilde{\boldsymbol{u}}_h^n\right).
\end{aligned}$$

Proof. Taking $\boldsymbol{v}_h = 2\Delta t\widetilde{\boldsymbol{u}}_h^n$ in (3.4), $\boldsymbol{C}_h = 2\Delta t\kappa\boldsymbol{B}_h^n$ in (3.5) and adding up the two equations, using $c\left(\widetilde{\boldsymbol{u}}_h^{n-1}, \widetilde{\boldsymbol{u}}_h^n, \widetilde{\boldsymbol{u}}_h^n\right) = 0$ and $2(a-b, a) = a^2 - b^2 + (a-b)^2$, there holds

$$\begin{aligned}
&\|\widetilde{\boldsymbol{u}}_h^n\|_0^2 - \left\|\mathscr{I}_h^T\boldsymbol{u}_h^{n-1}\right\|_0^2 + \left\|\widetilde{\boldsymbol{u}}_h^n - \mathscr{I}_h^T\boldsymbol{u}_h^{n-1}\right\|_0^2 + \kappa\left[\|\boldsymbol{B}_h^n\|_0^2 - \left\|\boldsymbol{B}_h^{n-1}\right\|_0^2 + \left\|\boldsymbol{B}_h^n - \boldsymbol{B}_h^{n-1}\right\|_0^2\right]\\
&+ 2\nu\Delta t\|\nabla\widetilde{\boldsymbol{u}}_h^n\|_0^2 + 2\kappa\Delta t R_m^{-1}\|\operatorname{curl}\boldsymbol{B}_h^n\|_0^2 + 2\Delta t\left(\mathscr{B}_h^T p_h^{n-1}, \widetilde{\boldsymbol{u}}_h^n\right) = 2\Delta t\left(\boldsymbol{f}^n, \widetilde{\boldsymbol{u}}_h^n\right).
\end{aligned} \tag{3.8}$$

By choosing $\boldsymbol{v}_{1h} = 2(\Delta t)^2\mathscr{C}_h^T p_h^{n-1}$ in (3.6) and applying $2(a-b,\ b) = a^2 - b^2 - (a-b)^2$, combining with (3.7), we can derive that

$$(\Delta t)^2\left[\left\|\mathscr{C}_h^T p_h^n\right\|_0^2 - \left\|\mathscr{C}_h^T p_h^{n-1}\right\|_0^2 - \left\|\mathscr{C}_h^T p_h^n - \mathscr{C}_h^T p_h^{n-1}\right\|_0^2\right] = 2\Delta t\left(\mathscr{I}_h\widetilde{\boldsymbol{u}}_h^n, \mathscr{C}_h^T p_h^{n-1}\right). \tag{3.9}$$

Thanks to Lemma 2, there holds

$$\left(\mathscr{I}_h\widetilde{\boldsymbol{u}}_h^n, \mathscr{C}_h^T p_h^{n-1}\right) = \left(\widetilde{\boldsymbol{u}}_h^n, \mathscr{I}_h^T\mathscr{C}_h^T p_h^{n-1}\right) = \left(\widetilde{\boldsymbol{u}}_h^n, \mathscr{B}_h^T p_h^{n-1}\right). \tag{3.10}$$

In addition, for any $\boldsymbol{v}_{1h} \in \boldsymbol{Z}_h$, we can rewrite (3.6) as follows

$$\boldsymbol{u}_h^n + \Delta t\left(\mathscr{C}_h^T p_h^n - \mathscr{C}_h^T p_h^{n-1}\right) = \mathscr{I}_h\widetilde{\boldsymbol{u}}_h^n. \tag{3.11}$$

Taking square on both sides of (3.11) and by (3.7), we can obtain

$$\|\boldsymbol{u}_h^n\|_0^2 + (\Delta t)^2\left\|\mathscr{C}_h^T p_h^n - \mathscr{C}_h^T p_h^{n-1}\right\|_0^2 = \|\mathscr{I}_h\widetilde{\boldsymbol{u}}_h^n\|_0^2. \tag{3.12}$$

Plugging (3.9) into (3.8), using (3.10) and (3.12), and noting that $\|\mathscr{I}_h\widetilde{\boldsymbol{u}}_h^n\|_0^2 = \|\widetilde{\boldsymbol{u}}_h^n\|_0^2$, we have

$$\begin{aligned}
&\|\boldsymbol{u}_h^n\|_0^2 - \left\|\mathscr{I}_h^T\boldsymbol{u}_h^{n-1}\right\|_0^2 + \left\|\widetilde{\boldsymbol{u}}_h^n - \mathscr{I}_h^T\boldsymbol{u}_h^{n-1}\right\|_0^2 + \kappa\|\boldsymbol{B}_h^n\|_0^2 - \kappa\left\|\boldsymbol{B}_h^{n-1}\right\|_0^2 + \kappa\left\|\boldsymbol{B}_h^n - \boldsymbol{B}_h^{n-1}\right\|_0^2\\
&+ 2\nu\Delta t\|\nabla\widetilde{\boldsymbol{u}}_h^n\|_0^2 + 2\kappa\Delta t R_m^{-1}\|\operatorname{curl}\boldsymbol{B}_h^n\|_0^2 + 2(\Delta t)^2\left(\left\|\mathscr{C}_h^T p_h^n\right\|_0^2 - \left\|\mathscr{C}_h^T p_h^{n-1}\right\|_0^2\right) = 2\Delta t\left(\boldsymbol{f}^n, \widetilde{\boldsymbol{u}}_h^n\right).
\end{aligned} \tag{3.13}$$

Summing up (3.13) from $n = 1$ to m, so we can conclude the proof. ■

4 | ERROR ANALYSIS OF THE FULLY DISCRETE MHD SYSTEM

In this section, we will establish the error estimates for the numerical solution $\left(\boldsymbol{u}_h^n, p_h^n, \boldsymbol{B}_h^n\right)$. Particularly, we are concerned with the $\boldsymbol{H}(\textbf{curl})$-conforming edge elements for discretizing magnetic induction $\boldsymbol{B}$ which may be not in $\boldsymbol{H}^1(\Omega)$. Some new techniques need to be developed in the subsequent analysis.

To obtain the optimal error estimate for pressure, we need to give an elaborate and fine estimate for the error of velocity and magnetic fields.

We will use a discrete version of the Gronwall inequality in a slightly more general form than the traditional one in the literature, and its detailed proof can be found in [59].

Lemma 4 (*Gronwall lemma*) *Let C_*, Δt, a_n, b_n, c_n and d_n be non-negative numbers with $n \geq 0$ such that*

$$a_m + \Delta t\sum_{n=0}^{m} b_n \leq \Delta t\sum_{n=0}^{m-1} d_n a_n + \Delta t\sum_{n=0}^{m} c_n + C_* \qquad \forall m \geq 0.$$

For all $\Delta t > 0$, then

$$a_m + \Delta t\sum_{n=0}^{m} b_n \leq \exp\left(\Delta t\sum_{n=0}^{m-1} d_n\right)\left\{\Delta t\sum_{n=0}^{m} c_n + C_*\right\} \qquad \forall m \geq 0.$$

In order to obtain the error estimates for all variables, we need to make the following regularity assumption for the weak solution of (2.10)–(2.11).

Assumption 1 Suppose that solution $(\boldsymbol{u}, p, \boldsymbol{B})$ satisfies the following regularity,

$$\begin{aligned}
&\boldsymbol{u} \in L^{\infty}\left(0,T;\boldsymbol{H}^{s+1}(\Omega)\cap \boldsymbol{H}^2(\Omega)\right), \ \boldsymbol{u}_t \in L^2\left(0,T;\boldsymbol{H}^s(\Omega)\right)\cap L^{\infty}\left(0,T;\boldsymbol{H}^2(\Omega)\right),\\
&\boldsymbol{u}_{tt} \in L^2\left(0,T;\boldsymbol{H}^{-1}(\Omega)\right), \qquad p \in L^{\infty}\left(0,T;H^s(\Omega)\cap H^1(\Omega)\right),\\
&p_t \in L^{\infty}\left(0,T;H^1(\Omega)\right), \qquad \boldsymbol{B} \in L^{\infty}\left(0,T;\boldsymbol{H}^s(\Omega)\right), \qquad \boldsymbol{B}_t \in L^2\left(0,T;\boldsymbol{H}^s(\Omega)\right),\\
&\boldsymbol{B}_{tt} \in L^2\left(0,T;\boldsymbol{L}^2(\Omega)\right), \qquad \mathrm{curl}\boldsymbol{B} \in L^2\left(0,T;\boldsymbol{H}^s(\Omega)\right),
\end{aligned}$$

where the exponent $s > 1/2$ depends on the regularity of the domain Ω.

Remark 6 Here, the regularity assumption of $\boldsymbol{B}$ is weaker than [39, 40] and it is minimal in the sense that it is satisfied by the strongest singularities of the Maxwell operator in polyhedral domains, compare [42, 43], which are often used in the analysis of finite element methods for incompressible MHD problems, see [2, 45] and the references therein. The regularity assumption on $\boldsymbol{u}$, $\boldsymbol{u}_t$ and p_t is the same as [36, 37, 39, 40] and the references therein. We can not weaken it since the Chorin projection method decouples the pressure from the momentum equation and it usually amounts to solve a Poisson type equation with the pressure p as unknown. It is very difficult to get an error estimate for Poisson problem with only $\boldsymbol{H}^s$ $(1/2 < s < 1)$ assumption. On the other hand, we have to use the $\boldsymbol{H}^2$ regularity assumption on $\boldsymbol{u}$ since it needs an estimate the H^1 stability of Stokes projection operator $Q_h p$ in the later proof.

To facilitate the subsequent analysis, we will assume there exists a constant $\mathrm{C_f}$ depends on $\boldsymbol{f}$, $\boldsymbol{u}^0$, $\boldsymbol{B}^0$ and Ω such that

$$\begin{aligned}
&\|\boldsymbol{u}\|_{L^{\infty}\left(0,T;\boldsymbol{H}^{1+s}(\Omega)\cap\boldsymbol{H}^2(\Omega)\right)} + \|\boldsymbol{u}_t\|_{L^2(0,T;\boldsymbol{H}^s(\Omega))\cap L^{\infty}\left(0,T;\boldsymbol{H}^2(\Omega)\right)}\\
&\quad + \|p\|_{L^{\infty}\left(0,T;H^s(\Omega)\cap H^1(\Omega)\right)} + \|p_t\|_{L^{\infty}\left(0,T;H^1(\Omega)\right)} + \|\boldsymbol{u}_{tt}\|_{L^2\left(0,T;\boldsymbol{H}^{-1}(\Omega)\right)} + \|\mathrm{curl}\boldsymbol{B}\|_{L^2(0,T;\boldsymbol{H}^s(\Omega))}\\
&\quad + \|\boldsymbol{B}\|_{L^{\infty}(0,T;\boldsymbol{H}^s(\Omega))} + \|\boldsymbol{B}_t\|_{L^2(0,T;\boldsymbol{H}^s(\Omega))} + \|\boldsymbol{B}_{tt}\|_{L^2\left(0,T;\boldsymbol{L}^2(\Omega)\right)} \leq C_f. \qquad (4.1)
\end{aligned}$$

We first introduce the Stokes projections: given $(\boldsymbol{u}, p) \in (\boldsymbol{X}_0 \times M)$, for any $(\boldsymbol{v}_h, q_h) \in (\boldsymbol{X}_h \times M_h)$, find $\mathcal{P}_h\boldsymbol{u} \in \boldsymbol{X}_h$ and $\mathcal{Q}_h p \in M_h$ such that

$$\nu (\nabla \mathcal{P}_h\boldsymbol{u}, \nabla \boldsymbol{v}_h) + \left(\mathscr{B}_h^T \mathcal{Q}_h p, \boldsymbol{v}_h\right) - (\mathscr{B}_h \mathcal{P}_h\boldsymbol{u}, q_h) = \nu (\nabla \boldsymbol{u}, \nabla \boldsymbol{v}_h) - (p, \operatorname{div} \boldsymbol{v}_h) + (q_h, \operatorname{div} \boldsymbol{u}). \tag{4.2}$$

We need to define the Fortin operator $\mathcal{F}_h$ from $\boldsymbol{W}_0$ to $\boldsymbol{W}_h$ (cf. [60]): given $\boldsymbol{B} \in \boldsymbol{W}_0$, for any $\boldsymbol{C}_h \in \boldsymbol{W}_h$ and $\psi_h \in S_h \subset H_0^1(\Omega)$, find $\mathcal{F}_h\boldsymbol{B} \in \boldsymbol{W}_h$ such that

$$R_m^{-1} (\operatorname{curl} \mathcal{F}_h\boldsymbol{B}, \operatorname{curl} \boldsymbol{C}_h) = R_m^{-1} (\operatorname{curl} \boldsymbol{B}, \operatorname{curl} \boldsymbol{C}_h), \qquad (\mathcal{F}_h\boldsymbol{B}, \nabla \psi_h) = (\boldsymbol{B}, \nabla \psi_h). \tag{4.3}$$

We suppose these projection operators satisfy the following approximation properties (see, e.g., [37, 58]),

$$\begin{aligned} h^{-1} \|\boldsymbol{u} - \mathcal{P}_h\boldsymbol{u}\|_0 + \|\boldsymbol{u} - \mathcal{P}_h\boldsymbol{u}\|_{1,2} + \|p - \mathcal{Q}_h p\|_0 &\le C_e h^{\ell} \left[\|\boldsymbol{u}\|_{\ell+1,2} + \|p\|_{\ell,2}\right], \\ \|\boldsymbol{B} - \mathcal{F}_h\boldsymbol{B}\|_0 + \|\operatorname{curl} (\boldsymbol{B} - \mathcal{F}_h\boldsymbol{B})\|_0 &\le C_e h^{\ell} \left[\|\boldsymbol{B}\|_{\ell,2} + \|\operatorname{curl} \boldsymbol{B}\|_{\ell,2}\right], \end{aligned} \tag{4.4}$$

with $\ell = \min\{k, s\}$, where $k \geq 1$ is the order index of the finite element spaces, $s > 1/2$ is the index of regularity of the exact solution and C_e is a generic constant depending on the regularity of the domain Ω. Note that the highest approximation error order for L^2 norm and $\boldsymbol{H}(\text{curl})$ norm of the chosen Nédélec finite element space are both order k, see, for example, [50, 53].

Assume that the initial values have a good approximation, namely:

$$\left\|\boldsymbol{B}(t_0) - \boldsymbol{B}_h^0\right\|_0^2 + \left\|\boldsymbol{u}(t_0) - \boldsymbol{u}_h^0\right\|_0^2 + (\Delta t)^2 \left\|\mathscr{C}_h^T \left(p(t_0) - p_h^0\right)\right\|_0^2 \le C h^{2\ell} + C(\Delta t)^2. \tag{4.5}$$

In addition, we can deduce the uniform stability of the projection operators by using inverse inequality (3.2) and Assumption 1. That is to say, there exists a constant $C_r > 0$ depending on the regularity of mesh such that

$$\begin{aligned} \|\mathcal{P}_h\boldsymbol{u}\|_{0,\infty} + \|\mathcal{P}_h\boldsymbol{u}\|_{1,3} &\le C_r \left(\|\boldsymbol{u}\|_{\ell+1,2} + \|p\|_{\ell,2}\right), \\ \|\mathcal{F}_h\boldsymbol{B}\|_{0,3} + \|\operatorname{curl} \mathcal{F}_h\boldsymbol{B}\|_{0,3} &\le C_r \left(\|\boldsymbol{B}\|_{\ell,2} + \|\operatorname{curl} \boldsymbol{B}\|_{\ell,2}\right). \end{aligned} \tag{4.6}$$

Furthermore, the projection $\mathcal{Q}_h p$ satisfies the following stability result, and this detailed proof can be found in Lemma 5.3 of [37].

Lemma 5 *Provided p is in $L^r(0, T; H^1(\Omega) \cap M)$ and $\boldsymbol{u}$ is in $L^r(0, T; \boldsymbol{H}^2(\Omega) \cap \boldsymbol{X})$, for $1 \le r \le \infty$, we have*

$$\left\|\mathscr{C}_h^T \mathcal{Q}_h p\right\|_{L^r(0,T;\boldsymbol{L}^2(\Omega))} \le C \left[\|p\|_{L^r(0,T;H^1(\Omega))} + \|\boldsymbol{u}\|_{L^r(0,T;\boldsymbol{H}^2(\Omega))}\right]. \tag{4.7}$$

In order to facilitate the subsequent error estimates, we define the following notations,

$$\begin{aligned} &\eta_{\tilde{\boldsymbol{u}}}^n = \mathcal{P}_h\boldsymbol{u}^n - \tilde{\boldsymbol{u}}_h^n, \qquad \eta_{\boldsymbol{u}}^n = \mathcal{P}_h\boldsymbol{u}^n - \boldsymbol{u}_h^n, \qquad \eta_p^n = \mathcal{Q}_h p^n - p_h^n, \\ &\eta_{\tilde{p}}^n = \mathcal{Q}_h p^n - p_h^{n-1}, \qquad \eta_{\boldsymbol{B}}^n = \mathcal{F}_h\boldsymbol{B}^n - \boldsymbol{B}_h^n. \end{aligned}$$

Combining (2.10)–(2.11), (3.4)–(3.7) and (4.2)–(4.3) together, we can derive the following error equations:

$$\begin{cases} \left(\frac{\eta_{\tilde{\boldsymbol{u}}}^n - \mathscr{I}_h^T \eta_{\boldsymbol{u}}^{n-1}}{\Delta t}, \boldsymbol{v}_h\right) + c\left(\eta_{\tilde{\boldsymbol{u}}}^{n-1}, \mathcal{P}_h\boldsymbol{u}^n, \boldsymbol{v}_h\right) + c\left(\tilde{\boldsymbol{u}}_h^{n-1}, \eta_{\tilde{\boldsymbol{u}}}^n, \boldsymbol{v}_h\right) + \nu\left(\nabla \eta_{\tilde{\boldsymbol{u}}}^n, \nabla \boldsymbol{v}_h\right) \\ \quad + \left(\mathscr{B}_h^T \eta_{\tilde{p}}^n, \boldsymbol{v}_h\right) + \kappa\left(\eta_{\boldsymbol{B}}^{n-1} \times \operatorname{curl} \mathcal{F}_h\boldsymbol{B}^n, \boldsymbol{v}_h\right) + \kappa\left(\boldsymbol{B}_h^{n-1} \times \operatorname{curl} \eta_{\boldsymbol{B}}^n, \boldsymbol{v}_h\right) = \left(R_1^n, \boldsymbol{v}_h\right), & (4.8) \\ \left(d_t \eta_{\boldsymbol{B}}^n, \boldsymbol{C}_h\right) + R_m^{-1}\left(\operatorname{curl} \eta_{\boldsymbol{B}}^n, \operatorname{curl} \boldsymbol{C}_h\right) - \left(\tilde{\boldsymbol{u}}_h^n \times \eta_{\boldsymbol{B}}^{n-1}, \operatorname{curl} \boldsymbol{C}_h\right) - \left(\eta_{\tilde{\boldsymbol{u}}}^n \times \mathcal{F}_h\boldsymbol{B}^{n-1}, \operatorname{curl} \boldsymbol{C}_h\right) = \left(R_2^n, \boldsymbol{C}_h\right), & (4.9) \end{cases}$$

and

$$\begin{cases} \left(\frac{\eta_{\boldsymbol{u}}^n - \mathcal{I}_h \eta_{\widetilde{\boldsymbol{u}}}^n}{\Delta t}, \boldsymbol{v}_{1h}\right) + \left(\mathscr{C}_h^T \left(\eta_p^n - \eta_{\widetilde{p}}^n\right), \boldsymbol{v}_{1h}\right) = 0, & (4.10)\\ (\mathscr{C}_h \eta_{\boldsymbol{u}}^n, q_h) = 0, & (4.11) \end{cases}$$

where

$$\begin{aligned}
&\left(R_1^n, \boldsymbol{v}_h\right)\\
&\quad = (d_t \mathcal{P}_h \boldsymbol{u}^n - d_t \boldsymbol{u}^n, \boldsymbol{v}_h) - \frac{1}{\Delta t}\int_{t_{n-1}}^{t_n} (t - t_{n-1})(\partial_{tt}\boldsymbol{u}, \boldsymbol{v}_h)\, dt\\
&\qquad - c\left(\boldsymbol{u}^n - \boldsymbol{u}^{n-1}, \boldsymbol{u}^n, \boldsymbol{v}_h\right) - c\left(\mathcal{P}_h \boldsymbol{u}^{n-1}, \boldsymbol{u}^n - \mathcal{P}_h \boldsymbol{u}^n, \boldsymbol{v}_h\right)\\
&\qquad - c\left(\boldsymbol{u}^{n-1} - \mathcal{P}_h \boldsymbol{u}^{n-1}, \boldsymbol{u}^n, \boldsymbol{v}_h\right) - \kappa\left(\left[\boldsymbol{B}^n - \boldsymbol{B}^{n-1}\right] \times \mathrm{curl}\, \boldsymbol{B}^n, \boldsymbol{v}_h\right)\\
&\qquad - \kappa\left(\mathcal{F}_h \boldsymbol{B}^{n-1} \times \mathrm{curl}\,(\boldsymbol{B}^n - \mathcal{F}_h \boldsymbol{B}^n), \boldsymbol{v}_h\right) - \kappa\left(\left[\boldsymbol{B}^{n-1} - \mathcal{F}_h \boldsymbol{B}^{n-1}\right] \times \mathrm{curl}\, \boldsymbol{B}^n, \boldsymbol{v}_h\right),\\
&\left(R_2^n, \boldsymbol{C}_h\right)\\
&\quad = (d_t \mathcal{F}_h \boldsymbol{B}^n - d_t \boldsymbol{B}^n, \boldsymbol{C}_h) - \frac{1}{\Delta t}\int_{t_{n-1}}^{t_n} (t - t_{n-1})(\partial_{tt}\boldsymbol{B}, \boldsymbol{C}_h)\, dt\\
&\qquad + \left(\left[\boldsymbol{u}^n - \mathcal{P}_h \boldsymbol{u}^n\right] \times \boldsymbol{B}^{n-1}, \mathrm{curl}\, \boldsymbol{C}_h\right) + \left(\boldsymbol{u}^n \times \left[\boldsymbol{B}^n - \boldsymbol{B}^{n-1}\right], \mathrm{curl}\, \boldsymbol{C}_h\right)\\
&\qquad + \left(\mathcal{P}_h \boldsymbol{u}^n \times \left[\boldsymbol{B}^{n-1} - \mathcal{F}_h \boldsymbol{B}^{n-1}\right], \mathrm{curl}\, \boldsymbol{C}_h\right).
\end{aligned}$$

Now, we estimate the residual terms R_1^n and R_2^n, which will be needed for the error analysis later.

Lemma 6 *Suppose* Assumption 1 *holds, with* $\ell = \min\{k, s\}$, *for all* $1 \le m \le N$, *the following estimate is established,*

$$\Delta t \sum_{n=1}^{m} \left(\left\|R_1^n\right\|_{-1,2}^2 + \left\|R_2^n\right\|_{\boldsymbol{H}(\mathrm{curl};\Omega)'}^2\right) \le C(\Delta t)^2 + Ch^{2\ell}. \tag{4.12}$$

Proof. In view of (2.6)–(2.9), (4.4) and Hölder inequality, it follows from the definition of R_1^n that

$$\begin{aligned}
&\left\|R_1^n\right\|_{-1,2}\\
&\quad \le C(\Delta t)^{1/2}\left\{\left(\int_{t_{n-1}}^{t_n} \|\partial_{tt}\boldsymbol{u}\|_{-1,2}^2\, dt\right)^{1/2} + \|\boldsymbol{u}^n\|_{1+\ell,2}\left(\int_{t_{n-1}}^{t_n} \|\boldsymbol{u}_t\|_0^2\, dt\right)^{1/2}\right.\\
&\qquad \left. + \|\mathrm{curl}\, \boldsymbol{B}^n\|_{0,3}\left(\int_{t_{n-1}}^{t_n} \|\boldsymbol{B}_t\|_0^2\, dt\right)^{1/2}\right\} + Ch^\ell \|d_t \boldsymbol{u}^n\|_{\ell,2}\\
&\qquad + 2Ch^\ell \left\|\mathcal{P}_h \boldsymbol{u}^{n-1}\right\|_{0,3} \|\boldsymbol{u}^n\|_{1+\ell,2} + 2Ch^\ell \left\|\boldsymbol{u}^{n-1}\right\|_{1+\ell,2} \|\nabla \boldsymbol{u}^n\|_0\\
&\qquad + Ch^\ell \|\mathrm{curl}\, \boldsymbol{B}^n\|_{\ell,2} \left\|\mathcal{F}_h \boldsymbol{B}^{n-1}\right\|_{0,3} + Ch^\ell \left\|\boldsymbol{B}^{n-1}\right\|_0 \|\mathrm{curl}\, \boldsymbol{B}^n\|_{0,3}.
\end{aligned}$$

Similarly, we can obtain

$$\begin{aligned}
&\left\|R_2^n\right\|_{\boldsymbol{H}(\mathrm{curl};\Omega)'}\\
&\quad \le C(\Delta t)^{1/2}\left\{\left(\int_{t_{n-1}}^{t_n} \|\partial_{tt}\boldsymbol{B}\|_0^2\, dt\right)^{1/2} + \|\boldsymbol{u}^n\|_{0,\infty}\left(\int_{t_{n-1}}^{t_n} \|\boldsymbol{B}_t\|_0^2\, dt\right)^{1/2}\right\}\\
&\qquad + Ch^\ell \|d_t \boldsymbol{B}^n\|_{\ell,2} + Ch^\ell \|\boldsymbol{u}^n\|_{1+\ell,2} \left\|\boldsymbol{B}^{n-1}\right\|_{0,3} + Ch^\ell \|\mathcal{P}_h \boldsymbol{u}^n\|_{0,\infty} \left\|\boldsymbol{B}^{n-1}\right\|_{\ell,2}.
\end{aligned}$$

Using Assumption 1 and (4.6), and summing up from $n = 1$ to m, the proof is completed. ∎

Under the condition of Assumption 1, we are now going to prove the following important convergence results.

Theorem 2 *Suppose that* Assumption 1 *is satisfied and there exists a positive constant* τ_0 *such that* $\Delta t \leq \tau_0$. *Let* $(\boldsymbol{u}^n, p^n, \boldsymbol{B}^n)$ *and* $\left(\boldsymbol{u}_h^n, \widetilde{\boldsymbol{u}}_h^n, p_h^n, \boldsymbol{B}_h^n\right)$ *be the solution of* (2.10)–(2.11) *and* (3.4)–(3.7), *respectively, for all* $N \geq m \geq 1$, *with* $\ell = \min\{k, s\}$, *we have*

$$\left\|\boldsymbol{u}^m - \boldsymbol{u}_h^m\right\|_0^2 + \|\boldsymbol{B}^m - \boldsymbol{B}_h^m\|_0^2 + \left\|\boldsymbol{u}^m - \widetilde{\boldsymbol{u}}_h^m\right\|_0^2 + (\Delta t)^2 \left\|\mathscr{C}_h^T \left(p^m - p_h^m\right)\right\|_0^2$$
$$+ \Delta t \sum_{n=1}^{m} \left(\nu \left\|\nabla\left(\boldsymbol{u}^n - \widetilde{\boldsymbol{u}}_h^n\right)\right\|_0^2 + R_m^{-1}\kappa \left\|\mathrm{curl}\left(\boldsymbol{B}^n - \boldsymbol{B}_h^n\right)\right\|_0^2 \right) \leq Ch^{2\ell} + C(\Delta t)^2.$$

Proof. By choosing $\boldsymbol{v}_h = 2\Delta t \eta_{\widetilde{\boldsymbol{u}}}^n \in \boldsymbol{X}_h$ in (4.8), $\boldsymbol{C}_h = 2\kappa\Delta t \eta_{\boldsymbol{B}}^n \in \boldsymbol{W}_{0h}^k$ in (4.9) and adding the two equations, we find

$$\begin{aligned}
&\|\eta_{\widetilde{\boldsymbol{u}}}^n\|_0^2 - \left\|\mathscr{I}_h^T \eta_{\boldsymbol{u}}^{n-1}\right\|_0^2 + \left\|\eta_{\widetilde{\boldsymbol{u}}}^n - \mathscr{I}_h^T \eta_{\boldsymbol{u}}^{n-1}\right\|_0^2 + \kappa\|\eta_{\boldsymbol{B}}^n\|_0^2 - \kappa\left\|\eta_{\boldsymbol{B}}^{n-1}\right\|_0^2 + \kappa\left\|\eta_{\boldsymbol{B}}^n - \eta_{\boldsymbol{B}}^{n-1}\right\|_0^2 \\
&+ 2\nu\Delta t\|\nabla\eta_{\widetilde{\boldsymbol{u}}}^n\|_0^2 + 2R_m^{-1}\kappa\Delta t\|\mathrm{curl}\,\eta_{\boldsymbol{B}}^n\|_0^2 + 2\Delta t c\left(\eta_{\widetilde{\boldsymbol{u}}}^{n-1}, \mathcal{P}_h\boldsymbol{u}^n, \eta_{\widetilde{\boldsymbol{u}}}^n\right) + 2\Delta t\kappa\left(\eta_{\boldsymbol{B}}^{n-1} \times \mathrm{curl}\,\mathcal{F}_h\boldsymbol{B}^n, \eta_{\widetilde{\boldsymbol{u}}}^n\right) \\
&- 2\Delta t\kappa\left(\mathcal{P}_h\boldsymbol{u}^n \times \eta_{\boldsymbol{B}}^{n-1}, \mathrm{curl}\,\eta_{\boldsymbol{B}}^n\right) + 2\Delta t\left(\mathscr{B}_h^T\eta_{\widetilde{p}}^n, \eta_{\widetilde{\boldsymbol{u}}}^n\right) = 2\Delta t\left(R_1^n, \eta_{\widetilde{\boldsymbol{u}}}^n\right) + 2\Delta t\kappa\left(R_2^n, \eta_{\boldsymbol{B}}^n\right),
\end{aligned} \tag{4.13}$$

where we have used the fact that

$$\left(\boldsymbol{B}_h^{n-1} \times \mathrm{curl}\,\eta_{\boldsymbol{B}}^n, \eta_{\widetilde{\boldsymbol{u}}}^n\right) - \left(\widetilde{\boldsymbol{u}}_h^{n-1} \times \eta_{\boldsymbol{B}}^{n-1}, \mathrm{curl}\,\eta_{\boldsymbol{B}}^n\right) - \left(\eta_{\widetilde{\boldsymbol{u}}}^n \times \mathcal{F}_h\boldsymbol{B}^{n-1}, \mathrm{curl}\,\eta_{\boldsymbol{B}}^n\right) = -\left(\mathcal{P}_h\boldsymbol{u}^n \times \eta_{\boldsymbol{B}}^{n-1}, \mathrm{curl}\,\eta_{\boldsymbol{B}}^n\right).$$

Taking $\boldsymbol{v}_{1h} = 2(\Delta t)^2\mathscr{C}_h^T\eta_{\widetilde{p}}^n \in \boldsymbol{Z}_h$ in (4.10), there holds

$$(\Delta t)^2\left[\left\|\mathscr{C}_h^T\eta_p^n\right\|_0^2 - \left\|\mathscr{C}_h^T\eta_{\widetilde{p}}^n\right\|_0^2 - \left\|\mathscr{C}_h^T\eta_p^n - \mathscr{C}_h^T\eta_{\widetilde{p}}^n\right\|_0^2\right] + 2\Delta t\left(\eta_{\boldsymbol{u}}^n - \mathscr{I}_h\eta_{\widetilde{\boldsymbol{u}}}^n, \mathscr{C}_h^T\eta_{\widetilde{p}}^n\right) = 0. \tag{4.14}$$

Combining (4.11) and (4.14) and using $\mathscr{I}_h^T\mathscr{C}_h^T = \mathscr{B}_h^T$, we have

$$(\Delta t)^2\left[\left\|\mathscr{C}_h^T\eta_p^n\right\|_0^2 - \left\|\mathscr{C}_h^T\eta_{\widetilde{p}}^n\right\|_0^2 - \left\|\mathscr{C}_h^T\eta_p^n - \mathscr{C}_h^T\eta_{\widetilde{p}}^n\right\|_0^2\right] = 2\Delta t\left(\eta_{\widetilde{\boldsymbol{u}}}^n, \mathscr{B}_h^T\eta_{\widetilde{p}}^n\right). \tag{4.15}$$

From (4.10), it can be seen that

$$\Delta t\left(\mathscr{C}_h^T\eta_p^n - \mathscr{C}_h^T\eta_{\widetilde{p}}^n\right) + \eta_{\boldsymbol{u}}^n = \mathscr{I}_h\eta_{\widetilde{\boldsymbol{u}}}^n. \tag{4.16}$$

By virtue of (4.11), there holds

$$(\Delta t)^2\left\|\mathscr{C}_h^T\eta_p^n - \mathscr{C}_h^T\eta_{\widetilde{p}}^n\right\|_0^2 + \|\eta_{\boldsymbol{u}}^n\|_0^2 = \|\mathscr{I}_h\eta_{\widetilde{\boldsymbol{u}}}^n\|_0^2. \tag{4.17}$$

Plugging (4.15) and (4.17) into (4.13), we can deduce

$$\begin{aligned}
&\|\eta_{\boldsymbol{u}}^n\|_0^2 - \left\|\mathscr{I}_h^T \eta_{\boldsymbol{u}}^{n-1}\right\|_0^2 + \left\|\eta_{\widetilde{\boldsymbol{u}}}^n - \mathscr{I}_h^T \eta_{\boldsymbol{u}}^{n-1}\right\|_0^2 + \kappa\|\eta_{\boldsymbol{B}}^n\|_0^2 - \kappa\left\|\eta_{\boldsymbol{B}}^{n-1}\right\|_0^2 + \kappa\left\|\eta_{\boldsymbol{B}}^n - \eta_{\boldsymbol{B}}^{n-1}\right\|_0^2 \\
&+ (\Delta t)^2\left[\left\|\mathscr{C}_h^T\eta_p^n\right\|_0^2 - \left\|\mathscr{C}_h^T\eta_{\widetilde{p}}^n\right\|_0^2\right] + 2\nu\Delta t\|\nabla\eta_{\widetilde{\boldsymbol{u}}}^n\|_0^2 + 2R_m^{-1}\kappa\Delta t\|\mathrm{curl}\,\eta_{\boldsymbol{B}}^n\|_0^2 + 2\Delta t c\left(\eta_{\widetilde{\boldsymbol{u}}}^{n-1}, \mathcal{P}_h\boldsymbol{u}^n, \eta_{\widetilde{\boldsymbol{u}}}^n\right) \\
&+ 2\Delta t\kappa\left(\eta_{\boldsymbol{B}}^{n-1} \times \mathrm{curl}\,\mathcal{F}_h\boldsymbol{B}^n, \eta_{\widetilde{\boldsymbol{u}}}^n\right) - 2\Delta t\kappa\left(\mathcal{P}_h\boldsymbol{u}^n \times \eta_{\boldsymbol{B}}^{n-1}, \mathrm{curl}\,\eta_{\boldsymbol{B}}^n\right) = 2\Delta t\left(R_1^n, \eta_{\widetilde{\boldsymbol{u}}}^n\right) + 2\Delta t\kappa\left(R_2^n, \eta_{\boldsymbol{B}}^n\right).
\end{aligned} \tag{4.18}$$

Applying the Young inequalities and (2.6)–(2.9), (3.1), and making use of (4.6) and $\left\|\operatorname{div}\eta_{\tilde{u}}^{n-1}\right\|_0 \le c_5\left\|\nabla\eta_{\tilde{u}}^{n-1}\right\|_0$, then the following estimates can be obtained

$$\begin{aligned}
2|c\left(\eta_{\tilde{u}}^{n-1},\mathcal{P}_h\boldsymbol{u}^n,\eta_{\tilde{u}}^n\right)| &= 2|\left(\left(\eta_{\tilde{u}}^{n-1}\cdot\nabla\right)\mathcal{P}_h\boldsymbol{u}^n,\eta_{\tilde{u}}^n\right)+\frac{1}{2}\left(\left(\operatorname{div}\eta_{\tilde{u}}^{n-1}\right)\mathcal{P}_h\boldsymbol{u}^n,\eta_{\tilde{u}}^n\right)|\\
&\le 2\left\|\eta_{\tilde{u}}^{n-1}\right\|_{0,6}\|\nabla\mathcal{P}_h\boldsymbol{u}^n\|_{0,3}\|\eta_{\tilde{u}}^n\|_0+\left\|\operatorname{div}\eta_{\tilde{u}}^{n-1}\right\|_0\|\mathcal{P}_h\boldsymbol{u}^n\|_{0,\infty}\|\eta_{\tilde{u}}^n\|_0\\
&\le \frac{2\nu}{4}\left\|\nabla\eta_{\tilde{u}}^{n-1}\right\|_0^2+4\nu^{-1}\left(c_1^2C_r^2C_f^2+c_5^2C_r^2C_f^2\right)\|\eta_{\tilde{u}}^n\|_0^2,\\
2|\kappa\left(\eta_{\boldsymbol{B}}^{n-1}\times\operatorname{curl}\mathcal{F}_h\boldsymbol{B}^n,\eta_{\tilde{u}}^n\right)| &\le 2\kappa\left\|\eta_{\boldsymbol{B}}^{n-1}\right\|_0\|\operatorname{curl}\mathcal{F}_h\boldsymbol{B}^n\|_{0,3}\|\eta_{\tilde{u}}^n\|_{0,6}\\
&\le \frac{\nu}{4}\|\nabla\eta_{\tilde{u}}^n\|_0^2+4\nu^{-1}\kappa^2c_1^2C_r^2C_f^2\left\|\eta_{\boldsymbol{B}}^{n-1}\right\|_0^2,
\end{aligned}$$

and

$$\begin{aligned}
&2\kappa|\left(\mathcal{P}_h\boldsymbol{u}^n\times\eta_{\boldsymbol{B}}^{n-1},\operatorname{curl}\eta_{\boldsymbol{B}}^n\right)| \le 2\kappa\|\mathcal{P}_h\boldsymbol{u}^n\|_{0,\infty}\left\|\eta_{\boldsymbol{B}}^{n-1}\right\|_0\|\operatorname{curl}\eta_{\boldsymbol{B}}^n\|_0\\
&\quad\le \frac{R_m^{-1}\kappa}{2}\|\operatorname{curl}\eta_{\boldsymbol{B}}^n\|_0^2+2R_m\kappa C_r^2C_f^2\left\|\eta_{\boldsymbol{B}}^{n-1}\right\|_0^2,\\
&2|\left(R_1^n,\eta_{\tilde{u}}^n\right)+\kappa\left(R_2^n,\eta_{\boldsymbol{B}}^n\right)|\\
&\quad\le 4\nu^{-1}\|R_1^n\|_{-1,2}^2+2R_m\kappa c_*^2\|R_2^n\|_{\boldsymbol{H}(\operatorname{curl};\Omega)'}^2+\frac{\nu}{4}\|\nabla\eta_{\tilde{u}}^n\|_0^2+\frac{R_m^{-1}\kappa}{2}\|\operatorname{curl}\eta_{\boldsymbol{B}}^n\|_0^2.
\end{aligned}$$

Thanks to $\eta_{\tilde{p}}^n = \mathcal{Q}_hp^n - p_h^{n-1}$, by using (4.1), (4.4), (4.7) and the Young inequalities, we obtain

$$\begin{aligned}
(\Delta t)^2\left\|\mathscr{C}_h^T\eta_{\tilde{p}}^n\right\|_0^2 &= (\Delta t)^2\left\|\mathscr{C}_h^T\left[\mathcal{Q}_hp^n-\mathcal{Q}_hp^{n-1}\right]+\mathscr{C}_h^T\eta_p^{n-1}\right\|_0^2\\
&= (\Delta t)^2\left\|\mathscr{C}_h^T\left[\mathcal{Q}_hp^n-\mathcal{Q}_hp^{n-1}\right]\right\|_0^2+(\Delta t)^2\left\|\mathscr{C}_h^T\eta_p^{n-1}\right\|_0^2\\
&\quad+2(\Delta t)^2\left(\mathscr{C}_h^T\left[\mathcal{Q}_hp^n-\mathcal{Q}_hp^{n-1}\right],\mathscr{C}_h^T\eta_p^{n-1}\right)\\
&\le (\Delta t)^2\left\|\mathscr{C}_h^T\eta_p^{n-1}\right\|_0^2+C(\Delta t)^3\left\|\mathscr{C}_h^T\eta_p^{n-1}\right\|_0^2+C(\Delta t)^3.
\end{aligned}$$

Due to $\|\eta_{\boldsymbol{u}}^n\|_0^2 = \|\eta_{\boldsymbol{u}}^n-\mathscr{I}_h^T\eta_{\boldsymbol{u}}^n\|_0^2+\|\mathscr{I}_h^T\eta_{\boldsymbol{u}}^n\|_0^2$, there holds

$$\begin{aligned}
&\left\|\mathscr{I}_h^T\eta_{\boldsymbol{u}}^n\right\|_0^2-\left\|\mathscr{I}_h^T\eta_{\boldsymbol{u}}^{n-1}\right\|_0^2+\left\|\eta_{\boldsymbol{u}}^n-\mathscr{I}_h^T\eta_{\boldsymbol{u}}^n\right\|_0^2+\left\|\eta_{\tilde{u}}^n-\mathscr{I}_h^T\eta_{\boldsymbol{u}}^{n-1}\right\|_0^2+\kappa\|\eta_{\boldsymbol{B}}^n\|_0^2\\
&\quad-\kappa\left\|\eta_{\boldsymbol{B}}^{n-1}\right\|_0^2+\kappa\left\|\eta_{\boldsymbol{B}}^n-\eta_{\boldsymbol{B}}^{n-1}\right\|_0^2+(\Delta t)^2\left[\left\|\mathscr{C}_h^T\eta_p^n\right\|_0^2-\left\|\mathscr{C}_h^T\eta_p^{n-1}\right\|_0^2\right]\\
&\quad+\frac{2\nu\Delta t}{4}\|\nabla\eta_{\tilde{u}}^n\|_0^2+\nu\Delta t\|\nabla\eta_{\tilde{u}}^n\|_0^2+R_m^{-1}\kappa\Delta t\|\operatorname{curl}\eta_{\boldsymbol{B}}^n\|_0^2\\
&\le C\Delta t\left(\|R_1^n\|_{-1,2}^2+\|R_2^n\|_{\boldsymbol{H}(\operatorname{curl};\Omega)'}^2\right)+4\nu^{-1}\left(c_1^2C_r^2C_f^2+c_5^2C_r^2C_f^2\right)\Delta t\|\eta_{\tilde{u}}^n\|_0^2\\
&\quad+C\Delta t\left(\kappa\left\|\eta_{\boldsymbol{B}}^{n-1}\right\|_0^2+(\Delta t)^2\left\|\mathscr{C}_h^T\eta_p^{n-1}\right\|_0^2\right)+\frac{2\nu\Delta t}{4}\left\|\nabla\eta_{\tilde{u}}^{n-1}\right\|_0^2+C(\Delta t)^3.
\end{aligned}\tag{4.19}$$

Summing up (4.19) from $n = 1$ to m, noticing $\|\eta_{\tilde{u}}^n\|_0 \le \|\eta_{\tilde{u}}^n-\mathscr{I}_h^T\eta_{\boldsymbol{u}}^{n-1}\|_0+\|\mathscr{I}_h^T\eta_{\boldsymbol{u}}^{n-1}\|_0$ and setting $\widehat{C} = 4\nu^{-1}\left(c_1^2C_r^2C_f^2+c_5^2C_r^2C_f^2\right)$, we can obtain

$$\begin{aligned}
&\left\|\mathscr{I}_h^T\eta_{\boldsymbol{u}}^m\right\|_0^2+(\Delta t)^2\left\|\mathscr{C}_h^T\eta_p^m\right\|_0^2+\kappa\|\eta_{\boldsymbol{B}}^m\|_0^2+\frac{\nu\Delta t}{2}\|\nabla\eta_{\tilde{\boldsymbol{u}}}^m\|_0^2\\
&\quad+\sum_{n=1}^m\left(\kappa\left\|\eta_{\boldsymbol{B}}^n-\eta_{\boldsymbol{B}}^{n-1}\right\|_0^2+(1-\widehat{C}\Delta t)\left\|\eta_{\tilde{\boldsymbol{u}}}^n-\mathscr{I}_h^T\eta_{\boldsymbol{u}}^{n-1}\right\|_0^2\right.\\
&\quad\left.+\left\|\eta_{\boldsymbol{u}}^n-\mathscr{I}_h^T\eta_{\boldsymbol{u}}^n\right\|_0^2\right)+\Delta t\sum_{n=1}^m\left(\nu\|\nabla\eta_{\tilde{\boldsymbol{u}}}^n\|_0^2+R_m^{-1}\kappa\|\operatorname{curl}\eta_{\boldsymbol{B}}^n\|_0^2\right)\\
&\le\left\|\mathscr{I}_h^T\eta_{\boldsymbol{u}}^0\right\|_0^2+(\Delta t)^2\left\|\mathscr{C}_h^T\eta_p^0\right\|_0^2+\kappa\left\|\eta_{\boldsymbol{B}}^0\right\|_0^2+\frac{\nu\Delta t}{2}\left\|\nabla\eta_{\boldsymbol{u}}^0\right\|_0^2+C(\Delta t)^2\\
&\quad+C\Delta t\sum_{n=1}^m\left(\|R_1^n\|_{-1,2}^2+\|R_2^n\|_{\boldsymbol{H}(\operatorname{curl};\Omega)'}^2\right)+C\Delta t\sum_{n=0}^{m-1}\left(\left\|\mathscr{I}_h^T\eta_{\boldsymbol{u}}^n\right\|_0^2\right.\\
&\quad\left.+\kappa\|\eta_{\boldsymbol{B}}^n\|_0^2+(\Delta t)^2\left\|\mathscr{C}_h^T\eta_p^n\right\|_0^2+\frac{\nu\Delta t}{2}\|\nabla\eta_{\tilde{\boldsymbol{u}}}^n\|_0^2\right).
\end{aligned}\tag{4.20}$$

By using Lemma 4 and Lemma 6, applying (4.1), (4.5), and (4.6), and choosing $\Delta t\le 1/(2\widehat{C})$, then we derive the following estimates

$$\begin{aligned}
&\left\|\mathscr{I}_h^T\eta_{\boldsymbol{u}}^m\right\|_0^2+(\Delta t)^2\left\|\mathscr{C}_h^T\eta_p^m\right\|_0^2+\kappa\|\eta_{\boldsymbol{B}}^m\|_0^2+\frac{\nu\Delta t}{2}\|\nabla\eta_{\tilde{\boldsymbol{u}}}^m\|_0^2\\
&\quad+\sum_{n=1}^m\left(\kappa\left\|\eta_{\boldsymbol{B}}^n-\eta_{\boldsymbol{B}}^{n-1}\right\|_0^2+\frac{1}{2}\left\|\eta_{\tilde{\boldsymbol{u}}}^n-\mathscr{I}_h^T\eta_{\boldsymbol{u}}^{n-1}\right\|_0^2+\left\|\eta_{\boldsymbol{u}}^n-\mathscr{I}_h^T\eta_{\boldsymbol{u}}^n\right\|_0^2\right)\\
&\quad+\Delta t\sum_{n=1}^m\left(\nu\left\|\nabla\eta_{\tilde{\boldsymbol{u}}}^n\right\|_0^2+R_m^{-1}\kappa\|\operatorname{curl}\eta_{\boldsymbol{B}}^n\|_0^2\right)\le Ch^{2\ell}+C(\Delta t)^2.
\end{aligned}\tag{4.21}$$

Making use of $\|\eta_{\boldsymbol{u}}^m\|_0^2=\left\|\eta_{\boldsymbol{u}}^m-\mathscr{I}_h^T\eta_{\boldsymbol{u}}^m\right\|_0^2+\left\|\mathscr{I}_h^T\eta_{\boldsymbol{u}}^m\right\|_0^2$, there holds

$$\|\eta_{\boldsymbol{u}}^m\|_0^2\le Ch^{2\ell}+C(\Delta t)^2.\tag{4.22}$$

Thanks to $\left\|\eta_{\tilde{\boldsymbol{u}}}^m\right\|_0^2\le\left\|\eta_{\tilde{\boldsymbol{u}}}^m-\mathscr{I}_h^T\eta_{\boldsymbol{u}}^{m-1}\right\|_0^2+\left\|\eta_{\boldsymbol{u}}^{m-1}\right\|_0^2$, we come to

$$\left\|\eta_{\tilde{\boldsymbol{u}}}^m\right\|_0^2\le Ch^{2\ell}+C(\Delta t)^2.\tag{4.23}$$

By virtue of the triangle inequality and (4.4), then the proof of Theorem 2 can be finished. ∎

By using Theorem 2, we can show the following estimate in a standard way, which helps to estimate the error of pressure.

Lemma 7 *Assuming that the hypotheses of* Theorem 2 *is valid. For* $1\le m\le N$, *with* $\ell=\min\{k,s\}$, *we have the following estimate*

$$\sum_{n=1}^m\left\|\eta_{\boldsymbol{u}}^n-\eta_{\boldsymbol{u}}^{n-1}\right\|_0^2\le C\left[h^{2\ell}+(\Delta t)^2\right].$$

Proof. Thanks to (4.10)–(4.11), for any $\boldsymbol{v}_{1h}\in\boldsymbol{Z}_h$, we can derive that

$$\frac{\eta_{\boldsymbol{u}}^n-\eta_{\boldsymbol{u}}^{n-1}}{\Delta t}+\mathscr{C}_h^T\left(\eta_p^n-\eta_{\tilde{p}}^n\right)=\frac{\mathscr{I}_h\eta_{\tilde{\boldsymbol{u}}}^n-\eta_{\boldsymbol{u}}^{n-1}}{\Delta t}.\tag{4.24}$$

Taking square on both sides of (4.24) and using $\mathscr{C}_h^T \eta_{\boldsymbol{u}}^n = 0$, we deduce that

$$\left\|\eta_{\boldsymbol{u}}^n - \eta_{\boldsymbol{u}}^{n-1}\right\|_0^2 + (\Delta t)^2 \left\|\mathscr{C}_h^T \left(\eta_p^n - \eta_{\tilde{p}}^n\right)\right\|_0^2 = \left\|\mathscr{I}_h \eta_{\tilde{\boldsymbol{u}}}^n - \eta_{\boldsymbol{u}}^{n-1}\right\|_0^2. \tag{4.25}$$

Applying $\mathscr{I}_h^T \mathscr{I}_h = I$, where I is an identity operator, there holds

$$\left\|\mathscr{I}_h \eta_{\tilde{\boldsymbol{u}}}^n - \eta_{\boldsymbol{u}}^{n-1}\right\|_0^2 = \left\|\eta_{\tilde{\boldsymbol{u}}}^n - \mathscr{I}_h^T \eta_{\boldsymbol{u}}^{n-1}\right\|_0^2 + \left\|\eta_{\boldsymbol{u}}^{n-1} - \mathscr{I}_h^T \eta_{\boldsymbol{u}}^{n-1}\right\|_0^2, \tag{4.26}$$

which implies that

$$\left\|\eta_{\boldsymbol{u}}^n - \eta_{\boldsymbol{u}}^{n-1}\right\|_0^2 \le \left\|\eta_{\tilde{\boldsymbol{u}}}^n - \mathscr{I}_h^T \eta_{\boldsymbol{u}}^{n-1}\right\|_0^2 + \left\|\eta_{\boldsymbol{u}}^{n-1} - \mathscr{I}_h^T \eta_{\boldsymbol{u}}^{n-1}\right\|_0^2. \tag{4.27}$$

Combining (4.21) and (4.27), we obtain

$$\sum_{n=1}^m \left\|\eta_{\boldsymbol{u}}^n - \eta_{\boldsymbol{u}}^{n-1}\right\|_0^2 \le Ch^{2\ell} + C(\Delta t)^2, \tag{4.28}$$

which leads to the desired result. ■

With the help of the inf-sup condition (3.3), we can establish the following estimate for pressure, provided that the exact solution is slightly smooth.

Theorem 3 *Under the hypotheses of* Theorem 2, *for* $1 \le m \le N$, *with* $\ell = \min\{k, s\}$, *the approximate pressure given by the projection scheme* (4.8)–(4.11) *satisfies*

$$\Delta t \sum_{n=1}^m \left\|p^{n-1} - p_h^{n-1}\right\|_0^2 \le C\left(\frac{1}{\Delta t} + h^{-1}(\Delta t)^2\right)\left((\Delta t)^2 + h^{2\ell}\right).$$

Proof. Multiplying both sides of (4.10) by $\mathscr{I}_h^T$ and adding it to (4.8), by virtue of $\mathscr{I}_h^T \mathscr{C}_h^T = \mathscr{B}_h^T$, we obtain

$$\begin{aligned}
&\left(\frac{\mathscr{I}_h^T \eta_{\boldsymbol{u}}^n - \mathscr{I}_h^T \eta_{\boldsymbol{u}}^{n-1}}{\Delta t}, \boldsymbol{v}_h\right) + c\left(\eta_{\tilde{\boldsymbol{u}}}^{n-1}, \mathcal{P}_h \boldsymbol{u}^n, \boldsymbol{v}_h\right) + c\left(\tilde{\boldsymbol{u}}_h^{n-1}, \eta_{\tilde{\boldsymbol{u}}}^n, \boldsymbol{v}_h\right) + \nu\left(\nabla \eta_{\tilde{\boldsymbol{u}}}^n, \nabla \boldsymbol{v}_h\right) \\
&+ \left(\mathscr{B}_h^T \eta_{\tilde{p}}^n, \boldsymbol{v}_h\right) + \kappa\left(\eta_{\boldsymbol{B}}^{n-1} \times \operatorname{curl} \mathcal{F}_h \boldsymbol{B}^n, \boldsymbol{v}_h\right) + \kappa\left(\boldsymbol{B}_h^{n-1} \times \operatorname{curl} \eta_{\boldsymbol{B}}^n, \boldsymbol{v}_h\right) = \left(R_1^n, \boldsymbol{v}_h\right).
\end{aligned}$$

By using of the inf-sup condition (3.3), we derive

$$\begin{aligned}
\left\|\eta_{\tilde{p}}^n\right\|_0 \le{}& \frac{\|\eta_{\boldsymbol{u}}^n - \eta_{\boldsymbol{u}}^{n-1}\|_0}{\Delta t} + 2c_1^2 \left\|\nabla \eta_{\tilde{\boldsymbol{u}}}^{n-1}\right\|_0 \|\nabla \mathcal{P}_h \boldsymbol{u}^n\|_0 + \nu \|\nabla \eta_{\tilde{\boldsymbol{u}}}^n\|_0 \\
&+ 2c_1 \|\nabla \eta_{\tilde{\boldsymbol{u}}}^n\|_0 \left(\left\|\mathcal{P}_h \boldsymbol{u}^{n-1}\right\|_{0,3} + \left\|\eta_{\tilde{\boldsymbol{u}}}^{n-1}\right\|_{0,3}\right) + c_1 \kappa \left\|\eta_{\boldsymbol{B}}^{n-1}\right\|_0 \|\operatorname{curl} \mathcal{F}_h \boldsymbol{B}^n\|_{0,3} + \|R_1^n\|_{-1,2} \\
&+ c_1 \kappa \left(\left\|\mathcal{F}_h \boldsymbol{B}^{n-1}\right\|_{0,3} + C_{inv} h^{-1/2} \left\|\eta_{\boldsymbol{B}}^{n-1}\right\|_0\right) \|\operatorname{curl} \eta_{\boldsymbol{B}}^n\|_0 .
\end{aligned} \tag{4.29}$$

Combining Theorem 2, Lemma 3, Lemma 6, Lemma 7 and (4.6) together, there holds

$$\begin{aligned}
\Delta t \sum_{n=1}^m \left\|\eta_{\tilde{p}}^n\right\|_0^2 \le{}& \frac{1}{\Delta t} \sum_{n=1}^m \left\|\eta_{\boldsymbol{u}}^n - \eta_{\boldsymbol{u}}^{n-1}\right\|_0^2 + C\Delta t \sum_{n=1}^m \left(\|\operatorname{curl} \eta_{\boldsymbol{B}}^n\|_0^2 + \|\nabla \eta_{\tilde{\boldsymbol{u}}}^n\|_0^2\right) \\
&+ C\left((\Delta t)^2 + h^{2\ell}\right) + Ch^{-1}\left((\Delta t)^2 + h^{2\ell}\right) \Delta t \sum_{n=1}^m \|\operatorname{curl} \eta_{\boldsymbol{B}}^n\|_0^2 \\
\le{}& C\left(\frac{1}{\Delta t} + h^{-1}(\Delta t)^2\right)\left((\Delta t)^2 + h^{2\ell}\right).
\end{aligned}$$

Thanks to $\eta_{\tilde{p}}^n = \mathcal{Q}_h p^n - \mathcal{Q}_h p^{n-1} + \eta_p^{n-1}$ and (4.1), we derive

$$\begin{aligned}\left\|\eta_p^{n-1}\right\|_0 &\leq \left\|\eta_{\tilde{p}}^n\right\|_0 + \left\|\mathcal{Q}_h p^n - \mathcal{Q}_h p^{n-1}\right\|_0 \\ &\leq \left\|\eta_{\tilde{p}}^n\right\|_0 + Ch^{\ell}\left\|p^n\right\|_{\ell,2} + C\sqrt{\Delta t}\left\|p_t\right\|_{L^2(0,T;L^2(\Omega))}.\end{aligned} \tag{4.30}$$

It yields that

$$\Delta t\sum_{n=1}^{m}\left\|\eta_p^{n-1}\right\|_0^2 \leq \Delta t\sum_{n=1}^{m}\left\|\eta_{\tilde{p}}^n\right\|_0^2 + C(\Delta t)^2 + Ch^{2\ell}. \tag{4.31}$$

By using of the triangle inequality and (4.4), we can finish the proof. ■

In fact, the error estimate of pressure obtained from Theorem 3 is not optimal. Inspired by [36, 37], we can obtain the optimal error estimate of pressure by the incremental pressure correction scheme.

In order to facilitate the estimation of subsequent error increments, we introduce the following notations:

$$\varepsilon_{\boldsymbol{u}}^n = \eta_{\boldsymbol{u}}^n - \eta_{\boldsymbol{u}}^{n-1}, \qquad \varepsilon_{\tilde{\boldsymbol{u}}}^n = \eta_{\tilde{\boldsymbol{u}}}^n - \eta_{\tilde{\boldsymbol{u}}}^{n-1}, \qquad \varepsilon_{\boldsymbol{B}}^n = \eta_{\boldsymbol{B}}^n - \eta_{\boldsymbol{B}}^{n-1}, \qquad \varepsilon_p^n = \eta_p^n - \eta_p^{n-1}, \qquad \varepsilon_{\tilde{p}}^n = \eta_{\tilde{p}}^n - \eta_{\tilde{p}}^{n-1}.$$

In addition to the hypotheses of Assumption 1, we need to assume that

$$\boldsymbol{u}_{tt} \in L^2(0,T;\boldsymbol{H}^s(\Omega)) \cap L^\infty\left(0,T;\boldsymbol{H}^2(\Omega)\right), \qquad \boldsymbol{u}_{ttt} \in L^2\left(0,T;\boldsymbol{L}^2(\Omega)\right), \tag{4.32}$$

$$\boldsymbol{B}_{tt} \in L^2(0,T;\boldsymbol{H}^s(\Omega)), \qquad \boldsymbol{B}_{ttt} \in L^2\left(0,T;\boldsymbol{L}^2(\Omega)\right), \tag{4.33}$$

$$\operatorname{curl}\mathrm{B}_t \in L^2(0,T;\boldsymbol{H}^s(\Omega)), \qquad p_{tt} \in L^\infty\left(0,T;H^1(\Omega)\right). \tag{4.33}$$

We further assume that the first step incremental error in the projection algorithm satisfies the following estimates,

$$\left\|\varepsilon_{\boldsymbol{u}}^1\right\|_0^2 + \left\|\varepsilon_{\tilde{\boldsymbol{u}}}^1\right\|_0^2 + \kappa\left\|\varepsilon_{\boldsymbol{B}}^1\right\|_0^2 + (\Delta t)^2\left\|\mathscr{C}_h^T\varepsilon_p^1\right\|_0^2 + \nu\Delta t\left\|\nabla\varepsilon_{\tilde{\boldsymbol{u}}}^1\right\|_0^2 \leq C\Delta t\left[h^{2\ell} + (\Delta t)^2\right]. \tag{4.35}$$

Lemma 8 *Assume that the hypotheses of* Theorem 2 *and* (4.32)–(4.35) *are satisfied, with* $\ell = \min\{k,s\}$. *Provided that* $\Delta t \approx \mathcal{O}\left(h^{1/2}\right)$, *then the following estimate is established*

$$\left\|\eta_{\boldsymbol{u}}^n - \eta_{\boldsymbol{u}}^{n-1}\right\|_0 \leq C(\Delta t)^{1/2}\left(h^{\ell} + \Delta t\right).$$

Proof. Taking the difference of (4.8) with two consecutive indices, there holds

$$\begin{aligned}&\left(\frac{\varepsilon_{\tilde{\boldsymbol{u}}}^n - \mathscr{I}_h^T\varepsilon_{\boldsymbol{u}}^{n-1}}{\Delta t}, \boldsymbol{v}_h\right) + \nu\left(\nabla\varepsilon_{\tilde{\boldsymbol{u}}}^n, \nabla\boldsymbol{v}_h\right) + \left(\mathscr{B}_h^T\varepsilon_{\tilde{p}}^n, \boldsymbol{v}_h\right) + c\left(\varepsilon_{\tilde{\boldsymbol{u}}}^{n-1}, \mathcal{P}_h\boldsymbol{u}^n, \boldsymbol{v}_h\right) \\ &+ c\left(\widetilde{\boldsymbol{u}}_h^{n-2}, \varepsilon_{\tilde{\boldsymbol{u}}}^n, \boldsymbol{v}_h\right) + c\left(\eta_{\tilde{\boldsymbol{u}}}^{n-2}, \mathcal{P}_h\boldsymbol{u}^n - \mathcal{P}_h\boldsymbol{u}^{n-1}, \boldsymbol{v}_h\right) + c\left(\widetilde{\boldsymbol{u}}_h^{n-1} - \widetilde{\boldsymbol{u}}_h^{n-2}, \eta_{\tilde{\boldsymbol{u}}}^n, \boldsymbol{v}_h\right) \\ &+ \kappa\left(\eta_{\boldsymbol{B}}^{n-2} \times \operatorname{curl}\left(\mathcal{F}_h\boldsymbol{B}^n - \mathcal{F}_h\boldsymbol{B}^{n-1}\right), \boldsymbol{v}_h\right) + \kappa\left(\varepsilon_{\boldsymbol{B}}^{n-1} \times \operatorname{curl}\mathcal{F}_h\boldsymbol{B}^n, \boldsymbol{v}_h\right) + \kappa\left(\boldsymbol{B}_h^{n-1} \times \operatorname{curl}\varepsilon_{\boldsymbol{B}}^n, \boldsymbol{v}_h\right) \\ &+ \kappa\left(\left(\boldsymbol{B}_h^{n-1} - \boldsymbol{B}_h^{n-2}\right) \times \operatorname{curl}\eta_{\boldsymbol{B}}^{n-1}, \boldsymbol{v}_h\right) = \left(R_1^n - R_1^{n-1}, \boldsymbol{v}_h\right).\end{aligned} \tag{4.36}$$

Taking the difference of (4.10) and (4.11) with two consecutive indices, respectively, we obtain

$$\begin{aligned}&\left(\frac{\varepsilon_{\boldsymbol{u}}^n - \mathscr{I}_h\varepsilon_{\tilde{\boldsymbol{u}}}^n}{\Delta t}, \boldsymbol{v}_{1h}\right) + \left(\mathscr{C}_h^T\left(\varepsilon_p^n - \varepsilon_{\tilde{p}}^n\right), \boldsymbol{v}_{1h}\right) = 0, \\ &\left(\mathscr{C}_h\varepsilon_{\boldsymbol{u}}^n, q_h\right) = 0.\end{aligned} \tag{4.37}$$

Taking the difference of (4.9) with two consecutive indices, we can arrive at

$$\left(d_t\varepsilon_{\boldsymbol{B}}^n,\boldsymbol{C}_h\right)+R_m^{-1}\left(\operatorname{curl}\varepsilon_{\boldsymbol{B}}^n,\operatorname{curl}\boldsymbol{C}_h\right)-\left(\widetilde{\boldsymbol{u}}_h^{n-1}\times\varepsilon_{\boldsymbol{B}}^{n-1},\operatorname{curl}\boldsymbol{C}_h\right)-\left(\left(\widetilde{\boldsymbol{u}}_h^{n}-\widetilde{\boldsymbol{u}}_h^{n-1}\right)\times\eta_{\boldsymbol{B}}^{n-1},\operatorname{curl}\boldsymbol{C}_h\right)$$
$$-\left(\eta_{\widetilde{\boldsymbol{u}}}^{n-1}\times\left(\mathcal{F}_h\boldsymbol{B}^{n-1}-\mathcal{F}_h\boldsymbol{B}^{n-2}\right),\operatorname{curl}\boldsymbol{C}_h\right)-\left(\varepsilon_{\widetilde{\boldsymbol{u}}}^n\times\mathcal{F}_h\boldsymbol{B}^{n-1},\operatorname{curl}\boldsymbol{C}_h\right)=\left(R_2^n-R_2^{n-1},\boldsymbol{C}_h\right). \tag{4.38}$$

Choosing $\boldsymbol{v}_h=2\Delta t\varepsilon_{\widetilde{\boldsymbol{u}}}^n$ in (4.36), we readily derive

$$\begin{aligned}&\|\varepsilon_{\widetilde{\boldsymbol{u}}}^n\|_0^2-\left\|\mathcal{J}_h^T\varepsilon_{\boldsymbol{u}}^{n-1}\right\|_0^2+\left\|\varepsilon_{\widetilde{\boldsymbol{u}}}^n-\mathcal{J}_h^T\varepsilon_{\boldsymbol{u}}^{n-1}\right\|_0^2+2\nu\Delta t\|\nabla\varepsilon_{\widetilde{\boldsymbol{u}}}^n\|_0^2+2\Delta tc\left(\varepsilon_{\widetilde{\boldsymbol{u}}}^{n-1},\mathcal{P}_h\boldsymbol{u}^n,\varepsilon_{\widetilde{\boldsymbol{u}}}^n\right)\\&+2\Delta tc\left(\eta_{\widetilde{\boldsymbol{u}}}^{n-2},\mathcal{P}_h\boldsymbol{u}^n-\mathcal{P}_h\boldsymbol{u}^{n-1},\varepsilon_{\widetilde{\boldsymbol{u}}}^n\right)+2\Delta tc\left(\widetilde{\boldsymbol{u}}_h^{n-1}-\widetilde{\boldsymbol{u}}_h^{n-2},\eta_{\widetilde{\boldsymbol{u}}}^n,\varepsilon_{\widetilde{\boldsymbol{u}}}^n\right)\\&+2\Delta t\left(\mathcal{B}_h^T\varepsilon_{\widetilde{p}}^n,\varepsilon_{\widetilde{\boldsymbol{u}}}^n\right)+2\Delta t\kappa\left(\eta_{\boldsymbol{B}}^{n-2}\times\operatorname{curl}\left(\mathcal{F}_h\boldsymbol{B}^n-\mathcal{F}_h\boldsymbol{B}^{n-1}\right),\varepsilon_{\widetilde{\boldsymbol{u}}}^n\right)\\&+2\Delta t\kappa\left(\varepsilon_{\boldsymbol{B}}^{n-1}\times\operatorname{curl}\mathcal{F}_h\boldsymbol{B}^n,\varepsilon_{\widetilde{\boldsymbol{u}}}^n\right)+2\Delta t\kappa\left(\boldsymbol{B}_h^{n-1}\times\operatorname{curl}\varepsilon_{\boldsymbol{B}}^n,\varepsilon_{\widetilde{\boldsymbol{u}}}^n\right)\\&+2\Delta t\kappa\left(\left(\boldsymbol{B}_h^{n-1}-\boldsymbol{B}_h^{n-2}\right)\times\operatorname{curl}\eta_{\boldsymbol{B}}^{n-1},\varepsilon_{\widetilde{\boldsymbol{u}}}^n\right)=2\Delta t\left(R_1^n-R_1^{n-1},\varepsilon_{\widetilde{\boldsymbol{u}}}^n\right).\end{aligned} \tag{4.39}$$

Taking $\boldsymbol{v}_{1h}=2(\Delta t)^2\mathcal{C}_h^T\varepsilon_{\widetilde{p}}^n$ in (4.37), we have

$$(\Delta t)^2\left[\left\|\mathcal{C}_h^T\varepsilon_p^n\right\|_0^2-\left\|\mathcal{C}_h^T\varepsilon_{\widetilde{p}}^n\right\|_0^2-\left\|\mathcal{C}_h^T\varepsilon_p^n-\mathcal{C}_h^T\varepsilon_{\widetilde{p}}^n\right\|_0^2\right]+2\Delta t\left(\varepsilon_{\boldsymbol{u}}^n-\mathcal{J}_h\varepsilon_{\widetilde{\boldsymbol{u}}}^n,\mathcal{C}_h^T\varepsilon_{\widetilde{p}}^n\right)=0. \tag{4.40}$$

Combining (4.37) and (4.40) together and using $\mathcal{J}_h^T\mathcal{C}_h^T=\mathcal{B}_h^T$, we have

$$(\Delta t)^2\left[\left\|\mathcal{C}_h^T\varepsilon_p^n\right\|_0^2-\left\|\mathcal{C}_h^T\varepsilon_{\widetilde{p}}^n\right\|_0^2-\left\|\mathcal{C}_h^T\varepsilon_p^n-\mathcal{C}_h^T\varepsilon_{\widetilde{p}}^n\right\|_0^2\right]=2\Delta t\left(\varepsilon_{\widetilde{\boldsymbol{u}}}^n,\mathcal{B}_h^T\varepsilon_{\widetilde{p}}^n\right). \tag{4.41}$$

Thanks to (4.37), for any $\boldsymbol{v}_{1h}\in\boldsymbol{Z}_h$, we know

$$\Delta t\left(\mathcal{C}_h^T\varepsilon_p^n-\mathcal{C}_h^T\varepsilon_{\widetilde{p}}^n\right)+\varepsilon_{\boldsymbol{u}}^n=\mathcal{J}_h\varepsilon_{\widetilde{\boldsymbol{u}}}^n. \tag{4.42}$$

By virtue of (4.37), there holds

$$(\Delta t)^2\left\|\mathcal{C}_h^T\varepsilon_p^n-\mathcal{C}_h^T\varepsilon_{\widetilde{p}}^n\right\|_0^2+\|\varepsilon_{\boldsymbol{u}}^n\|_0^2=\|\mathcal{J}_h\varepsilon_{\widetilde{\boldsymbol{u}}}^n\|_0^2. \tag{4.43}$$

Choosing $\boldsymbol{C}_h=2\Delta t\kappa\varepsilon_{\boldsymbol{B}}{}^n$ in (4.38), we are able to deduce that

$$\begin{aligned}&\kappa\|\varepsilon_{\boldsymbol{B}}^n\|_0^2-\kappa\left\|\varepsilon_{\boldsymbol{B}}^{n-1}\right\|_0^2+\kappa\left\|\varepsilon_{\boldsymbol{B}}^n-\varepsilon_{\boldsymbol{B}}^{n-1}\right\|_0^2+2R_m^{-1}\kappa\Delta t\|\operatorname{curl}\varepsilon_{\boldsymbol{B}}^n\|_0^2-2\Delta t\kappa\left(\widetilde{\boldsymbol{u}}_h^{n-1}\times\varepsilon_{\boldsymbol{B}}^{n-1},\operatorname{curl}\varepsilon_{\boldsymbol{B}}^n\right)\\&-2\Delta t\kappa\left(\left(\widetilde{\boldsymbol{u}}_h^n-\widetilde{\boldsymbol{u}}_h^{n-1}\right)\times\eta_{\boldsymbol{B}}^{n-1},\operatorname{curl}\varepsilon_{\boldsymbol{B}}^n\right)-2\Delta t\kappa\left(\eta_{\widetilde{\boldsymbol{u}}}^{n-1}\times\left(\mathcal{F}_h\boldsymbol{B}^{n-1}-\mathcal{F}_h\boldsymbol{B}^{n-2}\right),\operatorname{curl}\varepsilon_{\boldsymbol{B}}^n\right)\\&-2\Delta t\kappa\left(\varepsilon_{\widetilde{\boldsymbol{u}}}^n\times\mathcal{F}_h\boldsymbol{B}^{n-1},\operatorname{curl}\varepsilon_{\boldsymbol{B}}^n\right)=2\Delta t\kappa\left(R_2^n-R_2^{n-1},\varepsilon_{\boldsymbol{B}}^n\right).\end{aligned} \tag{4.44}$$

An application of $\mathcal{J}_h^T\mathcal{J}_h=I$ shows that $\|\mathcal{J}_h\varepsilon_{\widetilde{\boldsymbol{u}}}^n\|_0^2=\|\varepsilon_{\widetilde{\boldsymbol{u}}}^n\|_0^2$. Combining (4.39), (4.41), (4.43) and (4.44), we have

$$\begin{aligned}&\|\varepsilon_{\boldsymbol{u}}^n\|_0^2-\left\|\mathcal{J}_h^T\varepsilon_{\boldsymbol{u}}^{n-1}\right\|_0^2+\left\|\varepsilon_{\widetilde{\boldsymbol{u}}}^n-\mathcal{J}_h^T\varepsilon_{\boldsymbol{u}}^{n-1}\right\|_0^2+\kappa\|\varepsilon_{\boldsymbol{B}}^n\|_0^2-\kappa\left\|\varepsilon_{\boldsymbol{B}}^{n-1}\right\|_0^2+\kappa\left\|\varepsilon_{\boldsymbol{B}}^n-\varepsilon_{\boldsymbol{B}}^{n-1}\right\|_0^2\\&+(\Delta t)^2\left[\left\|\mathcal{C}_h^T\varepsilon_p^n\right\|_0^2-\left\|\mathcal{C}_h^T\varepsilon_{\widetilde{p}}^n\right\|_0^2\right]+2\nu\Delta t\|\nabla\varepsilon_{\widetilde{\boldsymbol{u}}}^n\|_0^2+2R_m^{-1}\kappa\Delta t\|\operatorname{curl}\varepsilon_{\boldsymbol{B}}^n\|_0^2+2\Delta tc\left(\varepsilon_{\widetilde{\boldsymbol{u}}}^{n-1},\mathcal{P}_h\boldsymbol{u}^n,\varepsilon_{\widetilde{\boldsymbol{u}}}^n\right)\\&+2\Delta tc\left(\eta_{\widetilde{\boldsymbol{u}}}^{n-2},\mathcal{P}_h\boldsymbol{u}^n-\mathcal{P}_h\boldsymbol{u}^{n-1},\varepsilon_{\widetilde{\boldsymbol{u}}}^n\right)+2\Delta tc\left(\widetilde{\boldsymbol{u}}_h^{n-1}-\widetilde{\boldsymbol{u}}_h^{n-2},\eta_{\widetilde{\boldsymbol{u}}}^n,\varepsilon_{\widetilde{\boldsymbol{u}}}^n\right)\\&+2\Delta t\kappa\left(\eta_{\boldsymbol{B}}^{n-2}\times\operatorname{curl}\left(\mathcal{F}_h\boldsymbol{B}^n-\mathcal{F}_h\boldsymbol{B}^{n-1}\right),\varepsilon_{\widetilde{\boldsymbol{u}}}^n\right)+2\Delta t\kappa\left(\varepsilon_{\boldsymbol{B}}^{n-1}\times\operatorname{curl}\mathcal{F}_h\boldsymbol{B}^n,\varepsilon_{\widetilde{\boldsymbol{u}}}^n\right)\end{aligned}$$

$$
\begin{aligned}
&+2\Delta t\kappa\left(\left(\boldsymbol{B}_h^{n-1}-\boldsymbol{B}_h^{n-2}\right)\times\operatorname{curl}\eta_{\boldsymbol{B}}^{n-1},\varepsilon_{\tilde{\boldsymbol{u}}}^{n}\right)-2\Delta t\kappa\left(\widetilde{\boldsymbol{u}}_h^{n-1}\times\varepsilon_{\boldsymbol{B}}^{n-1},\operatorname{curl}\varepsilon_{\boldsymbol{B}}^{n}\right)\\
&-2\Delta t\kappa\left(\eta_{\tilde{\boldsymbol{u}}}^{n-1}\times\left(\mathcal{F}_h\boldsymbol{B}^{n-1}-\mathcal{F}_h\boldsymbol{B}^{n-2}\right),\operatorname{curl}\varepsilon_{\boldsymbol{B}}^{n}\right)-2\Delta t\kappa\left(\left(\mathcal{P}_h\boldsymbol{u}^{n}-\mathcal{P}_h\boldsymbol{u}^{n-1}\right)\times\eta_{\boldsymbol{B}}^{n-1},\operatorname{curl}\varepsilon_{\boldsymbol{B}}^{n}\right)\\
=\;&2\Delta t\left(R_1^n-R_1^{n-1},\varepsilon_{\tilde{\boldsymbol{u}}}^{n}\right)+2\Delta t\kappa\left(R_2^n-R_2^{n-1},\varepsilon_{\boldsymbol{B}}^{n}\right).
\end{aligned}
\tag{4.45}
$$

Applying Young inequalities, (2.6)–(2.9), (4.6) and $\Delta t\approx\mathcal{O}\left(h^{1/2}\right)$, there holds

$$
\begin{aligned}
&2|c\left(\varepsilon_{\tilde{\boldsymbol{u}}}^{n-1},\mathcal{P}_h\boldsymbol{u}^{n},\varepsilon_{\tilde{\boldsymbol{u}}}^{n}\right)|\\
&\le\left\|\varepsilon_{\tilde{\boldsymbol{u}}}^{n-1}\right\|_0\|\nabla\mathcal{P}_h\boldsymbol{u}^n\|_{0,3}\|\varepsilon_{\tilde{\boldsymbol{u}}}^{n}\|_{0,6}+\left\|\varepsilon_{\tilde{\boldsymbol{u}}}^{n-1}\right\|_0\|\mathcal{P}_h\boldsymbol{u}^n\|_{0,\infty}\|\nabla\varepsilon_{\tilde{\boldsymbol{u}}}^{n}\|_0\\
&\le\frac{2\nu}{13}\|\nabla\varepsilon_{\tilde{\boldsymbol{u}}}^{n}\|_0^2+13\nu^{-1}\left(c_1^2C_r^2C_f^2+C_r^2C_f^2\right)\left\|\varepsilon_{\tilde{\boldsymbol{u}}}^{n-1}\right\|_0^2,\\
&2|c\left(\eta_{\tilde{\boldsymbol{u}}}^{n-2},\mathcal{P}_h\boldsymbol{u}^{n}-\mathcal{P}_h\boldsymbol{u}^{n-1},\varepsilon_{\tilde{\boldsymbol{u}}}^{n}\right)|\\
&\le\left[c_1\left\|\mathcal{P}_h\boldsymbol{u}^n-\mathcal{P}_h\boldsymbol{u}^{n-1}\right\|_{1,3}+\left\|\mathcal{P}_h\boldsymbol{u}^n-\mathcal{P}_h\boldsymbol{u}^{n-1}\right\|_{0,\infty}\right]\left\|\eta_{\tilde{\boldsymbol{u}}}^{n-2}\right\|_0\|\nabla\varepsilon_{\tilde{\boldsymbol{u}}}^{n}\|_0\\
&\le\frac{2\nu}{13}\|\nabla\varepsilon_{\tilde{\boldsymbol{u}}}^{n}\|_0^2+13\nu^{-1}\left(c_1^2C_r^2C_f^2+C_r^2C_f^2\right)\left\|\eta_{\tilde{\boldsymbol{u}}}^{n-2}\right\|_0^2,
\end{aligned}
$$

$$
\begin{aligned}
&2|c\left(\widetilde{\boldsymbol{u}}_h^{n-1}-\widetilde{\boldsymbol{u}}_h^{n-2},\eta_{\tilde{\boldsymbol{u}}}^{n},\varepsilon_{\tilde{\boldsymbol{u}}}^{n}\right)|=2|c\left(\mathcal{P}_h\boldsymbol{u}^{n-1}-\mathcal{P}_h\boldsymbol{u}^{n-2}-\varepsilon_{\tilde{\boldsymbol{u}}}^{n-1},\eta_{\tilde{\boldsymbol{u}}}^{n},\varepsilon_{\tilde{\boldsymbol{u}}}^{n}\right)|\\
&\le2c_1\|\nabla\varepsilon_{\tilde{\boldsymbol{u}}}^{n}\|_0\left\|\mathcal{P}_h\boldsymbol{u}^{n-1}-\mathcal{P}_h\boldsymbol{u}^{n-2}\right\|_{0,3}\|\nabla\eta_{\tilde{\boldsymbol{u}}}^{n}\|_0\\
&\quad+\|\varepsilon_{\tilde{\boldsymbol{u}}}^{n}\|_{0,6}\left\|\varepsilon_{\tilde{\boldsymbol{u}}}^{n-1}\right\|_{0,3}\|\nabla\eta_{\tilde{\boldsymbol{u}}}^{n}\|_0+\|\nabla\varepsilon_{\tilde{\boldsymbol{u}}}^{n}\|_0\left\|\varepsilon_{\tilde{\boldsymbol{u}}}^{n-1}\right\|_{0,6}\|\eta_{\tilde{\boldsymbol{u}}}^{n}\|_{0,3}\\
&\le\frac{4\nu}{13}\|\nabla\varepsilon_{\tilde{\boldsymbol{u}}}^{n}\|_0^2+26\nu^{-1}c_1^2\left\|\mathcal{P}_h\boldsymbol{u}^{n-1}-\mathcal{P}_h\boldsymbol{u}^{n-2}\right\|_{0,3}^2\|\nabla\eta_{\tilde{\boldsymbol{u}}}^{n}\|_0^2\\
&\quad+26\nu^{-1}c_1^4\|\nabla\eta_{\tilde{\boldsymbol{u}}}^{n}\|_0^2\left\|\nabla\varepsilon_{\tilde{\boldsymbol{u}}}^{n-1}\right\|_0^2,
\end{aligned}
$$

$$
\begin{aligned}
&2\kappa|\left(\eta_{\boldsymbol{B}}^{n-2}\times\operatorname{curl}\left(\mathcal{F}_h\boldsymbol{B}^n-\mathcal{F}_h\boldsymbol{B}^{n-1}\right),\varepsilon_{\tilde{\boldsymbol{u}}}^{n}\right)|\\
&\le\frac{\nu}{13}\|\nabla\varepsilon_{\tilde{\boldsymbol{u}}}^{n}\|_0^2+13\nu^{-1}c_1^2\kappa^2\left\|\operatorname{curl}\left(\mathcal{F}_h\boldsymbol{B}^n-\mathcal{F}_h\boldsymbol{B}^{n-1}\right)\right\|_{0,3}^2\left\|\eta_{\boldsymbol{B}}^{n-2}\right\|_0^2,\\
&2\kappa|\left(\varepsilon_{\boldsymbol{B}}^{n-1}\times\operatorname{curl}\mathcal{F}_h\boldsymbol{B}^n,\varepsilon_{\tilde{\boldsymbol{u}}}^{n}\right)|\le2\kappa\left\|\varepsilon_{\tilde{\boldsymbol{u}}}^{n}\right\|_{0,6}\|\operatorname{curl}\mathcal{F}_h\boldsymbol{B}^n\|_{0,3}\left\|\varepsilon_{\boldsymbol{B}}^{n-1}\right\|_0\\
&\le\frac{\nu}{13}\|\nabla\varepsilon_{\tilde{\boldsymbol{u}}}^{n}\|_0^2+13\nu^{-1}c_1^2C_r^2C_f^2\kappa^2\left\|\varepsilon_{\boldsymbol{B}}^{n-1}\right\|_0^2,
\end{aligned}
$$

and

$$
\begin{aligned}
&2\kappa|\left(\left(\boldsymbol{B}_h^{n-1}-\boldsymbol{B}_h^{n-2}\right)\times\operatorname{curl}\eta_{\boldsymbol{B}}^{n-1},\varepsilon_{\tilde{\boldsymbol{u}}}^{n}\right)|\\
&=2\kappa|\left(\left(\mathcal{F}_h\boldsymbol{B}^{n-1}-\mathcal{F}_h\boldsymbol{B}^{n-2}-\varepsilon_{\boldsymbol{B}}^{n-1}\right)\times\operatorname{curl}\eta_{\boldsymbol{B}}^{n-1},\varepsilon_{\tilde{\boldsymbol{u}}}^{n}\right)|\\
&\le2\kappa\left\|\mathcal{F}_h\boldsymbol{B}^{n-1}-\mathcal{F}_h\boldsymbol{B}^{n-2}\right\|_{0,3}\left\|\operatorname{curl}\eta_{\boldsymbol{B}}^{n-1}\right\|_0\|\varepsilon_{\tilde{\boldsymbol{u}}}^{n}\|_{0,6}+2\kappa\left\|\varepsilon_{\boldsymbol{B}}^{n-1}\right\|_{0,3}\left\|\operatorname{curl}\eta_{\boldsymbol{B}}^{n-1}\right\|_0\|\varepsilon_{\tilde{\boldsymbol{u}}}^{n}\|_{0,6}\\
&\le\frac{2\nu}{13}\|\nabla\varepsilon_{\tilde{\boldsymbol{u}}}^{n}\|_0^2+13\nu^{-1}\kappa^2\left[c_1^2\left\|\mathcal{F}_h\boldsymbol{B}^{n-1}-\mathcal{F}_h\boldsymbol{B}^{n-2}\right\|_{0,3}^2+c_1^2C_{inv}^2h^{-1}\left\|\varepsilon_{\boldsymbol{B}}^{n-1}\right\|_0^2\right]\left\|\operatorname{curl}\eta_{\boldsymbol{B}}^{n-1}\right\|_0^2.
\end{aligned}
$$

By using (3.1) and Young inequalities, we derive

$$
\begin{aligned}
&2|\left(R_1^n-R_1^{n-1},\varepsilon_{\tilde{\boldsymbol{u}}}^{n}\right)+\kappa\left(R_2^n-R_2^{n-1},\varepsilon_{\boldsymbol{B}}^{n}\right)|\\
&\le13\nu^{-1}\left\|R_1^n-R_1^{n-1}\right\|_{-1,2}^2+5R_m\kappa c_*^2\left\|R_2^n-R_2^{n-1}\right\|_{\boldsymbol{H}(\mathrm{curl};\Omega)'}^2+\frac{\nu}{13}\|\nabla\varepsilon_{\tilde{\boldsymbol{u}}}^{n}\|_0^2+\frac{\kappa}{5R_m}\|\operatorname{curl}\varepsilon_{\boldsymbol{B}}^{n}\|_0^2.
\end{aligned}
$$

We continue to deduce

$$\begin{aligned}
2\kappa\left|\left(\widetilde{\boldsymbol{u}}_h^{n-1}\times\varepsilon_{\boldsymbol{B}}^{n-1},\operatorname{curl}\varepsilon_{\boldsymbol{B}}^n\right)\right| &= 2\kappa\left|\left(\left[\mathcal{P}_h\boldsymbol{u}^{n-1}-\eta_{\widetilde{\boldsymbol{u}}}^{n-1}\right]\times\varepsilon_{\boldsymbol{B}}^{n-1},\operatorname{curl}\varepsilon_{\boldsymbol{B}}^n\right)\right| \\
&\le 2\kappa\left\|\mathcal{P}_h\boldsymbol{u}^{n-1}\right\|_{0,\infty}\left\|\varepsilon_{\boldsymbol{B}}^{n-1}\right\|_0\left\|\operatorname{curl}\varepsilon_{\boldsymbol{B}}^n\right\|_0+2\kappa\left\|\eta_{\widetilde{\boldsymbol{u}}}^{n-1}\right\|_{0,\infty}\left\|\varepsilon_{\boldsymbol{B}}^{n-1}\right\|_0\left\|\operatorname{curl}\varepsilon_{\boldsymbol{B}}^n\right\|_0 \\
&\le \frac{2\kappa}{5R_m}\left\|\operatorname{curl}\varepsilon_{\boldsymbol{B}}^n\right\|_0^2+5R_m\kappa\left\|\varepsilon_{\boldsymbol{B}}^{n-1}\right\|_0^2\left[C_r^2C_f^2+c_1^2C_{inv}^2h^{-1}\left\|\nabla\eta_{\widetilde{\boldsymbol{u}}}^{n-1}\right\|_0^2\right],
\end{aligned}$$

and

$$2\kappa\left|\left(\mathcal{P}_h\left[\boldsymbol{u}^n-\boldsymbol{u}^{n-1}\right]\times\eta_{\boldsymbol{B}}^{n-1},\operatorname{curl}\varepsilon_{\boldsymbol{B}}^n\right)\right|\le\frac{\kappa}{5R_m}\left\|\operatorname{curl}\varepsilon_{\boldsymbol{B}}^n\right\|_0^2+5R_m\kappa C_r^2C_f^2\left\|\eta_{\boldsymbol{B}}^{n-1}\right\|_0^2,$$

$$\begin{aligned}
&2\kappa\left|\left(\eta_{\widetilde{\boldsymbol{u}}}^{n-1}\times\left(\mathcal{F}_h\boldsymbol{B}^{n-1}-\mathcal{F}_h\boldsymbol{B}^{n-2}\right),\operatorname{curl}\varepsilon_{\boldsymbol{B}}^n\right)\right| \\
&\quad\le 2\kappa c_1\left\|\operatorname{curl}\varepsilon_{\boldsymbol{B}}^n\right\|_0\left\|\nabla\eta_{\widetilde{\boldsymbol{u}}}^{n-1}\right\|_0\left\|\mathcal{F}_h\boldsymbol{B}^{n-1}-\mathcal{F}_h\boldsymbol{B}^{n-2}\right\|_{0,3} \\
&\quad\le\frac{\kappa}{5R_m}\left\|\operatorname{curl}\varepsilon_{\boldsymbol{B}}^n\right\|_0^2+5R_m\kappa c_1^2\left\|\mathcal{F}_h\boldsymbol{B}^{n-1}-\mathcal{F}_h\boldsymbol{B}^{n-2}\right\|_{0,3}^2\left\|\nabla\eta_{\widetilde{\boldsymbol{u}}}^{n-1}\right\|_0^2.
\end{aligned}$$

Thanks to $\varepsilon_{\widetilde{p}}^n=\eta_{\widetilde{p}}^n-\eta_{\widetilde{p}}^{n-1}$, by using (4.4), (4.7), (4.32)–(4.34) and Young inequalities, we arrive at

$$\begin{aligned}
&(\Delta t)^2\left\|\mathscr{C}_h^T\varepsilon_{\widetilde{p}}^n\right\|_0^2 \\
&\quad=(\Delta t)^2\left\|\mathscr{C}_h^T\left[\mathcal{Q}_hp^n-\mathcal{Q}_hp^{n-1}\right]-\mathscr{C}_h^T\left[\mathcal{Q}_hp^{n-1}-\mathcal{Q}_hp^{n-2}\right]+\mathscr{C}_h^T\varepsilon_p^{n-1}\right\|_0^2 \\
&\quad=(\Delta t)^2\left\|\mathscr{C}_h^T\left[\mathcal{Q}_hp^n-\mathcal{Q}_hp^{n-1}\right]-\mathscr{C}_h^T\left[\mathcal{Q}_hp^{n-1}-\mathcal{Q}_hp^{n-2}\right]\right\|_0^2+(\Delta t)^2\left\|\mathscr{C}_h^T\varepsilon_p^{n-1}\right\|_0^2 \\
&\qquad+2(\Delta t)^2\left(\mathscr{C}_h^T\left[\mathcal{Q}_hp^n-\mathcal{Q}_hp^{n-1}\right]-\mathscr{C}_h^T\left[\mathcal{Q}_hp^{n-1}-\mathcal{Q}_hp^{n-2}\right],\mathscr{C}_h^T\varepsilon_p^{n-1}\right) \\
&\quad\le(\Delta t)^2\left\|\mathscr{C}_h^T\varepsilon_p^{n-1}\right\|_0^2+C(\Delta t)^3\left\|\mathscr{C}_h^T\varepsilon_p^{n-1}\right\|_0^2+C(\Delta t)^4.
\end{aligned}$$

The following inequality will be used in the rest of the proof:

$$\begin{aligned}
\left\|w^n-2w^{n-1}+w^{n-2}\right\|_0^2&=\left\|\int_{t_{n-1}}^{t_n}(t_n-t)\,w_{tt}\,dt-\int_{t_{n-2}}^{t_{n-1}}(t_{n-1}-t)\,w_{tt}\,dt\right\|_0^2 \\
&\le C(\Delta t)^3\left[\|w_{tt}\|_{L^2\left(t_{n-1},t_n;L^2(\Omega)\right)}^2+\|w_{tt}\|_{L^2\left(t_{n-2},t_{n-1};L^2(\Omega)\right)}^2\right].
\end{aligned}$$

In the next step, we shall estimate $\left\|R_1^n-R_1^{n-1}\right\|_{-1,2}$. It is easy to see that

$$\left\|\frac{\boldsymbol{u}^n-2\boldsymbol{u}^{n-1}+\boldsymbol{u}^{n-2}}{\Delta t}-\left(\partial_t\boldsymbol{u}^n-\partial_t\boldsymbol{u}^{n-1}\right)\right\|_0^2\le C(\Delta t)^3\int_{t_{n-2}}^{t_n}\|\partial_{ttt}\boldsymbol{u}\|_0^2dt.$$

From the properties of projections (4.4), there holds

$$\begin{aligned}
&\left\|d_t\mathcal{P}_h\boldsymbol{u}^n-d_t\mathcal{P}_h\boldsymbol{u}^{n-1}-d_t\boldsymbol{u}^n+d_t\boldsymbol{u}^{n-1}\right\|_0 \\
&\quad\le C_eh^{\ell}(\Delta t)^{-1}\left\|\boldsymbol{u}^n-2\boldsymbol{u}^{n-1}+\boldsymbol{u}^{n-2}\right\|_{\ell,2}] \\
&\quad\le Ch^{\ell}(\Delta t)^{1/2}\left[\|\boldsymbol{u}_{tt}\|_{L^2\left(t_{n-1},t_n;\boldsymbol{H}^{\ell}(\Omega)\right)}+\|\boldsymbol{u}_{tt}\|_{L^2\left(t_{n-2},t_{n-1};\boldsymbol{H}^{\ell}(\Omega)\right)}\right], \\
&\left|c\left(\boldsymbol{u}^{n-1}-\boldsymbol{u}^{n-2},\boldsymbol{u}^n-\boldsymbol{u}^{n-1},\boldsymbol{v}_h\right)\right| \\
&\quad\le C\Delta t\left(\int_{t_{n-1}}^{t_n}\|\boldsymbol{u}_t\|_{1,2}^2\,dt\right)^{1/2}\left(\int_{t_{n-2}}^{t_{n-1}}\|\boldsymbol{u}_t\|_{1,2}^2\,dt\right)^{1/2}\|\boldsymbol{v}_h\|_{1,2},
\end{aligned}$$

$$|c\left(\boldsymbol{u}^n-2\boldsymbol{u}^{n-1}+\boldsymbol{u}^{n-2},\boldsymbol{u}^n,\boldsymbol{v}_h\right)|\leq C(\Delta t)^{3/2}[\|\boldsymbol{u}_{tt}\|_{L^2(t_{n-1},t_n;\boldsymbol{H}^{\ell}(\Omega))}$$
$$+\|\boldsymbol{u}_{tt}\|_{L^2(t_{n-2},t_{n-1};\boldsymbol{H}^{\ell}(\Omega))}]\left(\|\nabla\boldsymbol{u}^n\|_{0,3}+\|\boldsymbol{u}^n\|_{0,\infty}\right)\|\boldsymbol{v}_h\|_{1,2},$$

we can continue to obtain

$$|c\left(\mathcal{P}_h\boldsymbol{u}^{n-2},\boldsymbol{u}^n-\boldsymbol{u}^{n-1}-\mathcal{P}_h\boldsymbol{u}^n+\mathcal{P}_h\boldsymbol{u}^{n-1},\boldsymbol{v}_h\right)|$$
$$\leq 2C_eh^{\ell}\left[\|\boldsymbol{u}^n\|_{1+\ell,2}+\left\|\boldsymbol{u}^{n-1}\right\|_{1+\ell,2}\right]\left\|\mathcal{P}_h\boldsymbol{u}^{n-2}\right\|_{0,3}\|\boldsymbol{v}_h\|_{1,2}$$

and

$$|c\left(\mathcal{P}_h\boldsymbol{u}^{n-1}-\mathcal{P}_h\boldsymbol{u}^{n-2},\boldsymbol{u}^n-\mathcal{P}_h\boldsymbol{u}^n,\boldsymbol{v}_h\right)|$$
$$=|c\left(\mathcal{P}_h\boldsymbol{u}^{n-1}-\boldsymbol{u}^{n-1}-\mathcal{P}_h\boldsymbol{u}^{n-2}+\boldsymbol{u}^{n-2}+\boldsymbol{u}^{n-1}-\boldsymbol{u}^{n-2},\boldsymbol{u}^n-\mathcal{P}_h\boldsymbol{u}^n,\boldsymbol{v}_h\right)|$$
$$\leq C_eh^{\ell}\|\boldsymbol{u}^n\|_{1+\ell,2}\sqrt{\Delta t}\left\|\partial_t\boldsymbol{u}^{n-1}\right\|_{0,3}\|\boldsymbol{v}_h\|_{1,2}$$
$$+C_eh^{2\ell}\left(\left\|\boldsymbol{u}^{n-1}\right\|_{\ell+1,2}+\left\|\boldsymbol{u}^{n-2}\right\|_{\ell+1,2}\right)\|\boldsymbol{u}^n\|_{\ell+1,2}\|\boldsymbol{v}_h\|_{1,2}.$$

The derivation of other terms is similar. We can deduce the following estimate by using (4.1) and (4.32)–(4.34)

$$\Delta t\sum_{n=2}^{m}\left\|R_1^n-R_1^{n-1}\right\|_{-1,2}^2\leq C\Delta t\left[(\Delta t)^2+h^{2\ell}\right]. \tag{4.46}$$

Similarly,

$$\Delta t\sum_{n=2}^{m}\left\|R_2^n-R_2^{n-1}\right\|_{\boldsymbol{H}(\mathrm{curl};\Omega)'}^2\leq C\Delta t\left[(\Delta t)^2+h^{2\ell}\right]. \tag{4.47}$$

Based on the properties of projection (4.4), (4.1) and (4.32)–(4.34), we find

$$\left\|\mathcal{P}_h\boldsymbol{u}^n-\mathcal{P}_h\boldsymbol{u}^{n-1}\right\|_{1,2}$$
$$\leq Ch^{\ell}\Delta t\|\boldsymbol{u}_t\|_{L^2(t_{n-1},t_n;\boldsymbol{H}^{1+\ell}(\Omega))}+C\Delta t\|\boldsymbol{u}_t\|_{L^\infty(t_{n-1},t_n;\boldsymbol{H}^1(\Omega))},$$
$$\left\|\mathrm{curl}\,\mathcal{F}_h\boldsymbol{B}^{n-1}-\mathrm{curl}\,\mathcal{F}_h\boldsymbol{B}^{n-2}\right\|_{0,3}$$
$$\leq Ch^{\ell-1/2}\sqrt{\Delta t}\|\mathrm{curl}\,\boldsymbol{B}_t\|_{L^2(t_{n-2},t_{n-1};\boldsymbol{H}^{\ell}(\Omega))}+C\sqrt{\Delta t}\|\mathrm{curl}\,\boldsymbol{B}_t\|_{L^2(t_{n-2},t_{n-1};\boldsymbol{H}^{\ell}(\Omega))}.$$

Combining these estimates with (4.45) and applying Assumption 1, there holds

$$\|\varepsilon_{\boldsymbol{u}}^n\|_0^2-\left\|\varepsilon_{\boldsymbol{u}}^{n-1}\right\|_0^2+\left\|\varepsilon_{\tilde{\boldsymbol{u}}}^n-\mathscr{I}_h^T\varepsilon_{\boldsymbol{u}}^{n-1}\right\|_0^2+\kappa\left[\|\varepsilon_{\boldsymbol{B}}^n\|_0^2-\left\|\varepsilon_{\boldsymbol{B}}^{n-1}\right\|_0^2+\left\|\varepsilon_{\boldsymbol{B}}^n-\varepsilon_{\boldsymbol{B}}^{n-1}\right\|_0^2\right]$$
$$+(\Delta t)^2\left[\left\|\mathscr{C}_h^T\varepsilon_p^n\right\|_0^2-\left\|\mathscr{C}_h^T\varepsilon_p^{n-1}\right\|_0^2\right]+\nu\Delta t\left\|\nabla\varepsilon_{\tilde{\boldsymbol{u}}}^n\right\|_0^2+R_m^{-1}\kappa\Delta t\left\|\mathrm{curl}\,\varepsilon_{\boldsymbol{B}}^n\right\|_0^2$$
$$\leq C\Delta t\left(\left\|R_1^n-R_1^{n-1}\right\|_{-1,2}^2+\left\|R_2^n-R_2^{n-1}\right\|_{\boldsymbol{H}(\mathrm{curl};\Omega)'}^2\right)$$
$$+C\Delta t\left(1+h^{-1}\left\|\mathrm{curl}\,\eta_{\boldsymbol{B}}^{n-1}\right\|_0^2+h^{-1}\left\|\nabla\eta_{\tilde{\boldsymbol{u}}}^{n-1}\right\|_0^2\right)\left(\left\|\varepsilon_{\boldsymbol{u}}^{n-1}\right\|_0^2+\kappa\left\|\varepsilon_{\boldsymbol{B}}^{n-1}\right\|_0^2\right.$$
$$\left.+(\Delta t)^2\left\|\mathscr{C}_h^T\varepsilon_p^{n-1}\right\|_0^2\right)+C\Delta t\left(\left\|\varepsilon_{\tilde{\boldsymbol{u}}}^{n-1}\right\|_0^2+\left\|\eta_{\tilde{\boldsymbol{u}}}^{n-2}\right\|_0^2+\left\|\eta_{\boldsymbol{B}}^{n-1}\right\|_0^2\right)$$

$$+ C(\Delta t)^2 \left(\|\nabla \eta_{\tilde{\boldsymbol{u}}}^n\|_0^2 + \left\|\eta_{\boldsymbol{B}}^{n-2}\right\|_0^2 + \left\|\operatorname{curl} \eta_{\boldsymbol{B}}^{n-1}\right\|_0^2 + \left\|\nabla \eta_{\tilde{\boldsymbol{u}}}^{n-1}\right\|_0^2 \right)$$

$$+ C\Delta t \left\|\nabla \varepsilon_{\tilde{\boldsymbol{u}}}^{n-1}\right\|_0^2 \|\nabla \eta_{\tilde{\boldsymbol{u}}}^n\|_0^2 + C(\Delta t)^4, \tag{4.48}$$

where we have used the fact that $\left\|\mathcal{I}_h^T \eta_{\boldsymbol{u}}^n\right\|_0 \leq \|\eta_{\boldsymbol{u}}^n\|_0$. Summing up (4.48) from $n = 2$ to m, and applying $(a-b)^2 \leq 2a^2 + 2b^2$, (4.46)–(4.47) and Theorem 2, we obtain

$$\begin{aligned}
&\|\varepsilon_{\boldsymbol{u}}^m\|_0^2 + \kappa\left\|\varepsilon_{\boldsymbol{B}}^m\right\|_0^2 + (\Delta t)^2\left\|\mathcal{C}_h^T \varepsilon_p^m\right\|_0^2 + \sum_{n=2}^{m}\left(\kappa\left\|\varepsilon_{\boldsymbol{B}}^n - \varepsilon_{\boldsymbol{B}}^{n-1}\right\|_0^2\right.\\
&\left.+ \left\|\varepsilon_{\tilde{\boldsymbol{u}}}^n - \mathcal{I}_h^T \varepsilon_{\boldsymbol{u}}^{n-1}\right\|_0^2\right) + \Delta t \sum_{n=2}^{m}\left(\nu\left\|\nabla \varepsilon_{\tilde{\boldsymbol{u}}}^n\right\|_0^2 + R_m^{-1}\kappa\left\|\operatorname{curl} \varepsilon_{\boldsymbol{B}}^n\right\|_0^2\right)\\
&\leq \left\|\varepsilon_{\boldsymbol{u}}^1\right\|_0^2 + \kappa\left\|\varepsilon_{\boldsymbol{B}}^1\right\|_0^2 + (\Delta t)^2\left\|\mathcal{C}_h^T \varepsilon_p^1\right\|_0^2\\
&+ C\Delta t\left[h^{2\ell} + (\Delta t)^2\right] + C\Delta t\sum_{n=2}^{m}\left(1 + h^{-1}\left\|\operatorname{curl} \eta_{\boldsymbol{B}}^{n-1}\right\|_0^2 + h^{-1}\left\|\nabla \eta_{\tilde{\boldsymbol{u}}}^{n-1}\right\|_0^2\right)\left(\left\|\varepsilon_{\boldsymbol{u}}^{n-1}\right\|_0^2\right.\\
&\left.+ \left\|\varepsilon_{\boldsymbol{B}}^{n-1}\right\|_0^2 + (\Delta t)^2\left\|\mathcal{C}_h^T \varepsilon_p^{n-1}\right\|_0^2\right) + C\left[(\Delta t)^2 + h^{2\ell}\right]\sum_{n=2}^{m}\left\|\nabla \varepsilon_{\tilde{\boldsymbol{u}}}^{n-1}\right\|_0^2.
\end{aligned}$$

Making use of (4.35), Theorem 2, Gronwall Lemma 4, and $\Delta t \approx \mathcal{O}\left(h^{1/2}\right)$, we derive that

$$\begin{aligned}
&\|\varepsilon_{\boldsymbol{u}}^m\|_0^2 + \kappa\left\|\varepsilon_{\boldsymbol{B}}^m\right\|_0^2 + (\Delta t)^2\left\|\mathcal{C}_h^T \varepsilon_p^m\right\|_0^2\\
&+ \Delta t\sum_{n=2}^{m}\left(\nu\left\|\nabla \varepsilon_{\tilde{\boldsymbol{u}}}^n\right\|_0^2 + R_m^{-1}\kappa\left\|\operatorname{curl} \varepsilon_{\boldsymbol{B}}^n\right\|_0^2\right) \leq C\Delta t\left[h^{2\ell} + (\Delta t)^2\right].
\end{aligned}\tag{4.49}$$

Then Lemma 8 follows. ∎

Now, we are ready to give the optimal error estimate for pressure.

Theorem 4 *Under the hypotheses of* Lemma 8, *assume that* $\Delta t \approx \mathcal{O}\left(h^{1/2}\right)$. *For* $1 \leq m \leq N$, *with* $\ell = \min\{k, s\}$, *the approximate pressure given by the projection scheme* (4.8)–(4.11) *satisfies*

$$\Delta t \sum_{n=1}^{m}\left\|p^{n-1} - p_h^{n-1}\right\|_0^2 \leq C(\Delta t)^2 + Ch^{2\ell}.$$

Proof. Multiplying both sides of (4.10) by $\mathcal{I}_h^T$ and adding it to (4.8), by virtue of $\mathcal{I}_h^T\mathcal{C}_h^T = \mathcal{B}_h^T$, we obtain

$$\begin{aligned}
&\left(\frac{\mathcal{I}_h^T \eta_{\boldsymbol{u}}^n - \mathcal{I}_h^T \eta_{\boldsymbol{u}}^{n-1}}{\Delta t}, \boldsymbol{v}_h\right) + c\left(\eta_{\tilde{\boldsymbol{u}}}^{n-1}, \mathcal{P}_h \boldsymbol{u}^n, \boldsymbol{v}_h\right) + c\left(\tilde{\boldsymbol{u}}_h^{n-1}, \eta_{\tilde{\boldsymbol{u}}}^n, \boldsymbol{v}_h\right) + \nu\left(\nabla \eta_{\tilde{\boldsymbol{u}}}^n, \nabla \boldsymbol{v}_h\right)\\
&+ \left(\mathcal{B}_h^T \eta_p^n, \boldsymbol{v}_h\right) + \kappa\left(\eta_{\boldsymbol{B}}^{n-1} \times \operatorname{curl} \mathcal{F}_h \boldsymbol{B}^n, \boldsymbol{v}_h\right) + \kappa\left(\boldsymbol{B}_h^{n-1} \times \operatorname{curl} \eta_{\boldsymbol{B}}^n, \boldsymbol{v}_h\right) = \left(R_1^n, \boldsymbol{v}_h\right).
\end{aligned}$$

Utilizing the inf-sup condition (3.3), we derive that

$$\left\|\eta_{\tilde{p}}^{n}\right\|_0 \le \frac{\|\eta_{\tilde{u}}^{n}-\eta_{\tilde{u}}^{n-1}\|_0}{\Delta t} + 2c_1^2\left\|\nabla\eta_{\tilde{u}}^{n-1}\right\|_0\|\nabla\mathcal{P}_h\boldsymbol{u}^n\|_0 + \nu\left\|\nabla\eta_{\tilde{u}}^{n}\right\|_0 + 2c_1\left\|\nabla\eta_{\tilde{u}}^{n}\right\|_0\left(\left\|\mathcal{P}_h\boldsymbol{u}^{n-1}\right\|_{0,3}+\left\|\eta_{\tilde{u}}^{n-1}\right\|_{0,3}\right)$$
$$+c_1\kappa\left\|\eta_{\boldsymbol{B}}^{n-1}\right\|_0\|\mathrm{curl}\,\mathcal{F}_h\boldsymbol{B}^n\|_{0,3} + \left\|R_1^n\right\|_{-1,2} + c_1\kappa\left(\left\|\mathcal{F}_h\boldsymbol{B}^{n-1}\right\|_{0,3} + C_{inv}h^{-1/2}\left\|\eta_{\boldsymbol{B}}^{n-1}\right\|_0\right)\|\mathrm{curl}\,\eta_{\boldsymbol{B}}^{n}\|_0 .$$

Combining Theorem 2, Lemma 3, Lemma 6, Lemma 8, (4.6), and $\Delta t \approx \mathcal{O}\left(h^{1/2}\right)$, there holds

$$\Delta t\sum_{n=1}^{m}\left\|\eta_{\tilde{p}}^{n}\right\|_0^2 \le \frac{1}{\Delta t}\Delta t\left((\Delta t)^2+h^{2\ell}\right) + \Delta t\sum_{n=1}^{m}\left(\|\mathrm{curl}\,\eta_{\boldsymbol{B}}^{n}\|_0^2 + \|\nabla\eta_{\tilde{u}}^{n}\|_0^2\right)$$
$$+C\Delta t\left((\Delta t)^2+h^{2\ell}\right) + Ch^{-1}\left((\Delta t)^2+h^{2\ell}\right)\Delta t\sum_{n=1}^{m}\|\mathrm{curl}\,\eta_{\boldsymbol{B}}^{n}\|_0^2$$
$$\le C\left((\Delta t)^2+h^{2\ell}\right).$$

Due to $\eta_{\tilde{p}}^{n} = \mathcal{Q}_hp^n - \mathcal{Q}_hp^{n-1} + \eta_p^{n-1}$, we clearly see

$$\left\|\eta_p^{n-1}\right\|_0^2 \le \left\|\eta_{\tilde{p}}^{n}\right\|_0^2 + C(\Delta t)^2 + Ch^{2\ell}, \tag{4.50}$$

which means that

$$\Delta t\sum_{n=1}^{m}\left\|\eta_p^{n-1}\right\|_0^2 \le Ch^{2\ell} + C(\Delta t)^2. \tag{4.51}$$

By using of the triangle inequality and (4.4), then we finish the proof. ∎

Remark 7 There is a time-step size restriction in Theorem 4. It may be possible to remove such an CFL like condition by the new splitting technique developed in the literature, see, for example, [61–64]. To this end, we need to propose a proper time discrete system and derive its temporal error and spatial error independently. But so far we have not found such a suitable time discrete system and it is worthy of further exploration in the future.

5 | NUMERICAL EXPERIMENTS

In this section, we consider some numerical experiments to verify the convergence rate and performance of fully discrete projection finite element method for MHD system. We consider the particular case $\boldsymbol{Z}_h = \boldsymbol{X}_h + \nabla M_h$ with $M_h \in H^1(\Omega)$. Then it can be checked that the incremental pressure algorithm should be implemented as follows:

Step 1 Given $\tilde{\boldsymbol{u}}_h^{n-1}$, p_h^{n-1} and $\boldsymbol{B}_h^{n-1}$, for any $\boldsymbol{v}_h \in \boldsymbol{X}_h$ and $\boldsymbol{C}_h \in \boldsymbol{W}_h$, find $\tilde{\boldsymbol{u}}_h^{n} \in \boldsymbol{X}_h$ and $\boldsymbol{B}_h^{n} \in \boldsymbol{W}_h$ such that

$$\begin{cases}\left(\frac{\tilde{\boldsymbol{u}}_h^{n}-\boldsymbol{u}_h^{n-1}}{\Delta t},\boldsymbol{v}_h\right) + c\left(\tilde{\boldsymbol{u}}_h^{n-1},\tilde{\boldsymbol{u}}_h^{n},\boldsymbol{v}_h\right) + \nu\left(\nabla\tilde{\boldsymbol{u}}_h^{n},\nabla\boldsymbol{v}_h\right) - \left(p_h^{n-1},\mathrm{div}\,\boldsymbol{v}_h\right) \\ \quad +\kappa\left(\boldsymbol{B}_h^{n-1}\times\mathrm{curl}\,\boldsymbol{B}_h^{n},\boldsymbol{v}_h\right) = \left(\boldsymbol{f}^n,\boldsymbol{v}_h\right), & (5.1)\\ \left(d_t\boldsymbol{B}_h^{n},\boldsymbol{C}_h\right) + R_m^{-1}\left(\mathrm{curl}\,\boldsymbol{B}_h^{n},\mathrm{curl}\,\boldsymbol{C}_h\right) - \left(\tilde{\boldsymbol{u}}_h^{n}\times\boldsymbol{B}_h^{n-1},\mathrm{curl}\,\boldsymbol{C}_h\right) = 0. & (5.2)\end{cases}$$

TABLE 1 Convergence rates of Euler semi-implicit scheme at terminal time (Example 5.1)

Δt	$\Vert\mathcal{E}_u\Vert_0$	Order	$\Vert\mathcal{E}_u\Vert_{1,2}$	Order	$\Vert\mathcal{E}_p\Vert_0$	Order	$\Vert\mathcal{E}_B\Vert_0$	Order	$\Vert\mathcal{E}_B\Vert_{H(\mathrm{curl};\Omega)}$	Order
0.1000	1.453 e-04	-	1.486 e-03	-	1.076 e-02	-	8.566 e-04	-	4.180 e-03	-
0.0500	4.795 e-05	1.5991	4.964 e-04	1.5818	5.123 e-03	1.0707	4.182 e-04	1.0345	2.040 e-03	1.0352
0.0250	1.813 e-05	1.4035	1.706 e-04	1.5404	2.309 e-03	1.1501	2.065 e-04	1.0176	1.007 e-03	1.0178
0.0125	8.851 e-06	1.0343	7.848 e-05	1.1206	1.105 e-03	1.0628	1.026 e-04	1.0088	5.005 e-04	1.0089

Step 2 Given $\widetilde{\boldsymbol{u}}_h^n$ and p_h^{n-1}, for any $q_h \in M_h$, find $p_h^n \in M_h$ and $\boldsymbol{u}_h^n \in \boldsymbol{Z}_h$ such that

$$\begin{cases} \left(\nabla\left(p_h^n - p_h^{n-1}\right), \nabla q_h\right) = -\left(\frac{1}{\Delta t}\mathrm{div}\widetilde{\boldsymbol{u}}_h^n, q_h\right), & (5.3)\\ \boldsymbol{u}_h^n = \widetilde{\boldsymbol{u}}_h^n - \Delta t \nabla\left(p_h^n - p_h^{n-1}\right). & (5.4)\end{cases}$$

We develop the parallel code based on the finite element package-Parallel Hierarchical Grids (PHG), cf. [65, 66]. All computations are carried out on the LSSC-IV Cluster of the State Key Laboratory of Scientific and Engineering Computing, Chinese Academy of Sciences. The first two examples are used to verify the error estimates of the fully discrete projection finite element method. The last one is to simulate the three dimensional lid-driven cavity MHD flow in the presence of a transverse magnetic field. In all examples, the domain under consideration is $\Omega = (0, 1)^3$ and the finite element mesh is obtained by uniform tetrahedral partition. We employ the continuous P_2 elements for discretizing velocity $\boldsymbol{u}$, the continuous P_1 elements for discretizing pressure p and the second-order $\boldsymbol{H}(\mathbf{curl})$-conforming edge elements for discretizing magnetic induction $\boldsymbol{B}$. The approximation errors at the last moment $t_N = T$ are denoted by

$$\mathcal{E}_{\boldsymbol{u}} = \boldsymbol{u}(T) - \boldsymbol{u}_h^N, \qquad \mathcal{E}_{\boldsymbol{B}} = \boldsymbol{B}(T) - \boldsymbol{B}_h^N, \qquad \mathcal{E}_p = p(T) - p_h^N.$$

Example 5.1 This example is to validate the efficiency of the Euler semi-implicit scheme, when $\Delta t \to 0$. Set the physical parameters $\nu = 1$, $\kappa = 1$ and $R_m = 1$. The time interval is [0, 1]. We can choose the following exact solution

$$\boldsymbol{u} = \left(ye^{-t}, z\cos(t), x\right), \qquad p = 0, \qquad \boldsymbol{B} = \left(ye^{-t}, 0, 0\right).$$

It can be seen that the exact solution is linear in space, therefore, the temporal errors play a dominant role in the analysis. We fix a tetrahedral mesh with $h = 0.433$, the terminal time $T = 1$, and test the convergence rate at each time step. By the numerical experiment, Table 1 shows that the convergence rate of Euler semi-implicit scheme is first-order.

Example 5.2 This example is to test the convergence rate for Euler semi-implicit scheme when both timestep and meshwidth are refined at the same time. Set the parameters $\nu = 1$, $\kappa = 1$ and $R_m = 1$, the initial mesh size $h_0 = 0.433$ and the time interval [0, 1]. The analytic solution is chosen as

$$\boldsymbol{u} = (\sin(y)\sin(t), 0, 0), \qquad p = x + y + z - 1.5, \qquad \boldsymbol{B} = (0, \sin(x)\sin(t), 0).$$

By setting $\Delta t_0 = h_0^2$, Table 2 shows that the discrete solution has the asymptotic behaviors

$$\Vert\mathcal{E}_{\boldsymbol{u}}\Vert_{1,2} \approx \mathcal{O}\left(\Delta t + h^2\right), \qquad \Vert\mathcal{E}_{\boldsymbol{B}}\Vert_{\boldsymbol{H}(\mathrm{curl};\Omega)} \approx \mathcal{O}\left(\Delta t + h^2\right),$$
$$\Vert\mathcal{E}_{\boldsymbol{u}}\Vert_0 \approx \mathcal{O}\left(\Delta t + h^2\right), \qquad \Vert\mathcal{E}_{\boldsymbol{B}}\Vert_0 \approx \mathcal{O}\left(\Delta t + h^2\right), \qquad \Vert\mathcal{E}_p\Vert_0 \approx \mathcal{O}\left(\Delta t + h^2\right).$$

TABLE 2 The convergence rate of Euler semi-implicit scheme at terminal time (Example 5.2)

$(\Delta t, h)$	$\|\mathcal{E}_u\|_{1,2}$	$\|\mathcal{E}_B\|_{H(\mathrm{curl};\Omega)}$	$\|\mathcal{E}_p\|_0$	$\|\mathcal{E}_u\|_0$	$\|\mathcal{E}_B\|_0$
$(\Delta t_0, h_0)$	1.669 e-03	5.390 e-03	9.909 e-04	9.372 e-05	1.077 e-03
$(\Delta t_0/4, h_0/2)$	4.195 e-04	1.718 e-03	5.070 e-04	2.212 e-05	3.444 e-04
$(\Delta t_0/16, h_0/4)$	1.074 e-04	4.871 e-04	1.193 e-04	6.461 e-06	9.673 e-05
$(\Delta t_0/64, h_0/8)$	2.730 e-05	1.274 e-04	2.383 e-05	1.804 e-06	2.511 e-05

TABLE 3 The convergence rate of Euler semi-implicit scheme at terminal time (Example 5.2)

$(\Delta t, h)$	$\|\mathcal{E}_u\|_{1,2}$	$\|\mathcal{E}_B\|_{H(\mathrm{curl};\Omega)}$	$\|\mathcal{E}_p\|_0$	$\|\mathcal{E}_u\|_0$	$\|\mathcal{E}_B\|_0$
$(\Delta t_0, h_0)$	1.546 e-03	2.955 e-03	6.406 e-04	7.208 e-05	5.520 e-04
$(\Delta t_0/8, h_0/2)$	3.723 e-04	5.169 e-04	1.248 e-04	9.476 e-06	8.428 e-05
$(\Delta t_0/64, h_0/4)$	9.100 e-05	9.330 e-05	1.043 e-05	1.235 e-06	1.099 e-05
$(\Delta t_0/512, h_0/8)$	2.249 e-05	2.000 e-05	1.152 e-06	1.550 e-07	1.381 e-06

Clearly the optimal convergence rates are obtained for both temporal and spatial variables in Table 2.

By setting $\Delta t_0 = h_0^3$, Table 3 shows that the discrete solution has the asymptotic behaviors

$$\begin{aligned}
&\|\mathcal{E}_{\boldsymbol{u}}\|_{1,2} \approx \mathcal{O}\left(\Delta t + h^2\right), \qquad \|\mathcal{E}_{\boldsymbol{B}}\|_{\boldsymbol{H}(\mathrm{curl};\Omega)} \approx \mathcal{O}\left(\Delta t + h^2\right),\\
&\|\mathcal{E}_{\boldsymbol{u}}\|_0 \approx \mathcal{O}\left(\Delta t + h^3\right), \qquad \left\|\mathcal{E}_p\right\|_0 \approx \mathcal{O}\left(\Delta t + h^3\right), \qquad \|\mathcal{E}_{\boldsymbol{B}}\|_0 \approx \mathcal{O}\left(\Delta t + h^3\right).
\end{aligned}$$

Obviously, Table 3 shows the optimal convergence rates of temporal and spatial variables.

Table 2 demonstrates that the $\boldsymbol{L}^2$-error orders of velocity and magnetic induction, $\boldsymbol{H}^1$-error order of velocity and $\boldsymbol{H}$(curl)-error order of magnetic induction, and L^2-error order of pressure are all of the second-order accuracy in space, while Table 3 illustrates that the $\boldsymbol{L}^2$-error orders of velocity and magnetic induction are all of the third order accuracy in space. From Tables 2 and 3, we can see that the convergence rates agree well with the theoretical ones.

Example 5.3 This example computes the benchmark problem of driven cavity flow. The right-hand side of the momentum equation is given by $\boldsymbol{f} = (0, 0, 0)$. The physical parameters are set by $\nu^{-1} = R_e = 100$, $R_m = 100$ and $\kappa = 1$. The initial values are given by $\boldsymbol{B}^0 = (0, 1, 0)$, $\boldsymbol{u}^0 = (w, 0, 0)$, where $w \in C^1(\Omega)$ and satisfies

$$w(x, y, 1) = 1 \qquad \text{and} \qquad w(x, y, z) = 0 \quad \forall z \in [0, 1-h],$$

together with the following boundary conditions

$$\boldsymbol{u} = \boldsymbol{u}^0, \qquad \boldsymbol{B} \times \boldsymbol{n} = \boldsymbol{B}^0 \times \boldsymbol{n} \qquad \text{on } \partial\Omega.$$

The terminal time $T = 21.27$ is chosen such that the physical fields reach almost steady state, namely

$$\left\|\boldsymbol{u}_h^n - \boldsymbol{u}_h^{n-1}\right\|_0 + \left\|\boldsymbol{B}_h^n - \boldsymbol{B}_h^{n-1}\right\|_0 < 10^{-8}.$$

Figure 1 is the projection of velocity streamlines on the cross-section $y = 0.5$. Figure 2 shows the projection of the vortex streamlines curl $\boldsymbol{u_h}$ at $x = 0.5$ and $z = 0.5$, respectively, and they describe the vortex structure of the fluid. Figure 3 shows the distributions of magnetic induction $\boldsymbol{B}_h$ on three cross-sections $x = 0.5$, $y = 0.5$ and $z = 0.5$, respectively. Figure 4 shows the distributions of the kinetic

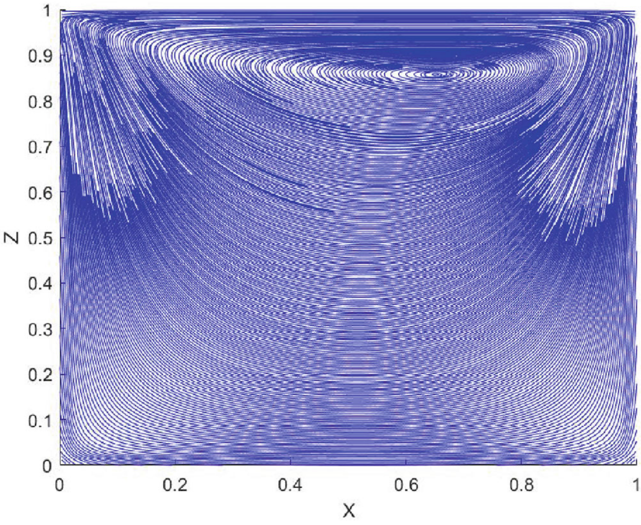

FIGURE 1 Streamlines of the velocity $\boldsymbol{u}_h$ on the cross-section $y = 0.5$

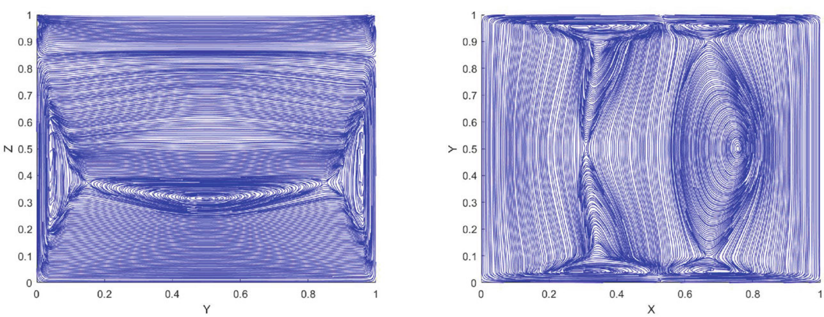

FIGURE 2 Two streamlines of the vortex at $x = 0.5$ and $z = 0.5$ respectively (from left to right)

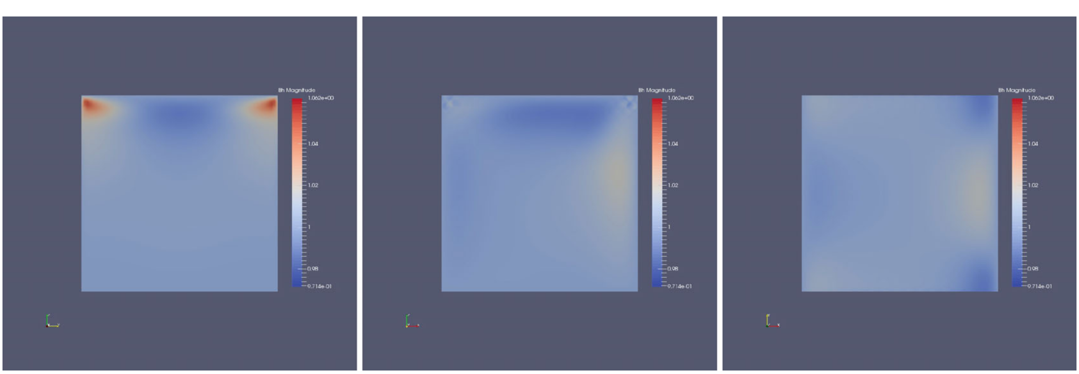

FIGURE 3 Distributions of magnetic induction. Left: $x = 0.5$. Middle: $y = 0.5$. Right: $z = 0.5$

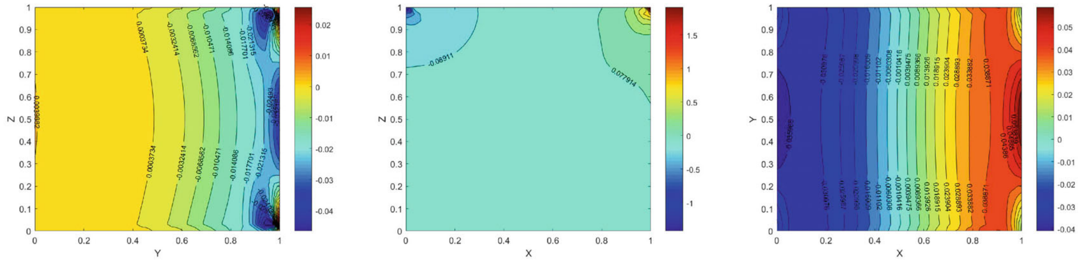

FIGURE 4 The contour of the pressure p_h. Left: $x = 0.5$. Middle: $y = 0.5$. Right: $z = 0.5$

pressure on three cross-sections $x = 0.5$, $y = 0.5$ and $z = 0.5$, respectively. In the middle figure, since the flow is driven from left to right, it generates high pressure regions near the right upper corner.

6 | SUMMARY

In this paper, we propose, analyze, and numerically illustrate a fully discrete projection method for the MHD model based on $\boldsymbol{H}(\mathbf{curl})$-conforming edge elements for discretizing magnetic induction $\boldsymbol{B}$. The proposed scheme can be used for the domain may be a non-convex polyhedra and the magnetic induction $\boldsymbol{B}$ has regularity lower than $\boldsymbol{H}^1(\Omega)$. Under the reasonable regularity hypothesis for the exact solution, we derive optimal error estimates for velocity and magnetic induction, while the error order of pressure is not optimal. However, when $\Delta t \approx \mathcal{O}\left(h^{1/2}\right)$, we can obtain the optimal estimate for pressure.

ACKNOWLEDGMENTS

The research was supported by National Natural Science Foundation of China (Nos 11871467, 12271514, 12201353) and Shandong Province Natural Science Foundation (ZR2021QA054).

DATA AVAILABILITY STATEMENT

Research data are not shared.

ORCID

Qianqian Ding https://orcid.org/0000-0003-1490-5786
Xiaoming He https://orcid.org/0000-0003-1270-4972
Shipeng Mao https://orcid.org/0000-0003-4115-6039

REFERENCES

[1] P. A. Davidson, *An introduction to magnetohydrodynamics*, Cambridge Texts in Applied Mathematics, Cambridge University Press, Cambridge, 2001.
[2] J. F. Gerbeau, C. Le Bris, and T. Lelièvre, *Mathematical methods for the magnetohydrodynamics of liquid metals*, Numerical Mathematics and Scientific Computation, Oxford University Press, Oxford, 2006.
[3] A. E. Lifschitz, *Magnetohydrodynamics and spectral theory*, Developments in Electromagnetic Theory and Applications, Vol 4, Kluwer Academic Publishers Group, Dordrecht, 1989.
[4] R. Moreau, *Magnetohydrodynamics*, Fluid Mechanics and its Applications, Vol 3, Kluwer Academic Publishers Group, Dordrecht, 1990 Translated from the French by A. F. Wright.
[5] Q. Ding, X. Long, and S. Mao, *Convergence analysis of Crank-Nicolson extrapolated fully discrete scheme for thermally coupled incompressible magnetohydrodynamic system*, Appl. Numer. Math. 157 (2020), 522–543. https://doi.org/10.1016/j.apnum.2020.06.018.

[6] K. Hu, Y. Ma, and J. Xu, *Stable finite element methods preserving $\nabla \cdot B = 0$ exactly for MHD models*, Numer. Math. 135 (2017), no. 2, 371–396. https://doi.org/10.1007/s00211-016-0803-4.
[7] M. Sermange and R. Temam, *Some mathematical questions related to the MHD equations*, Commun. Pure Appl. Math. 36 (1983), no. 5, 635–664. https://doi.org/10.1002/cpa.3160360506.
[8] Y. He, *Unconditional convergence of the Euler semi-implicit scheme for the three-dimensional incompressible MHD equations*, IMA J. Numer. Anal. 35 (2014), no. 2, 767–801.
[9] W. Layton, H. Tran, and C. Trenchea, *Numerical analysis of two partitioned methods for uncoupling evolutionary MHD flows*, Numer. Methods Partial Differ. Equ. 30 (2014), no. 4, 1083–1102.
[10] J. G. Liu and R. Pego, *Stable discretization of magnetohydrodynamics in bounded domains*, Commun. Math. Sci. 8 (2010), no. 1, 235–251.
[11] M. D. Gunzburger, A. J. Meir, and J. S. Peterson, *On the existence, uniqueness, and finite element approximation of solutions of the equations of stationary, incompressible magnetohydrodynamics*, Math. Comput. 56 (1991), no. 194, 523–563.
[12] N. B. Salah, A. Soulaimani, and W. G. Habashi, *A finite element method for magnetohydrodynamics*, Comput. Methods Appl. Mech. Eng. 190 (2001), no. 43, 5867–5892.
[13] E. G. Phillips, J. N. Shadid, E. C. Cyr, H. C. Elman, and R. P. Pawlowski, *Block preconditioners for stable mixed nodal and edge finite element representations of incompressible resistive MHD*, SIAM J. Sci. Comput. 38 (2016), no. 6, B1009–B1031.
[14] S. Badia, R. Planas, and J. V. Gutiérrez-Santacreu, *Unconditionally stable operator splitting algorithms for the incompressible magnetohydrodynamics system discretized by a stabilized finite element formulation based on projections*, Int. J. Numer. Methods Eng. 93 (2013), no. 3, 302–328.
[15] Y. Ma, K. Hu, X. Hu, and J. Xu, *Robust preconditioners for incompressible MHD models*, J. Comput. Phys. 316 (2016), 721–746.
[16] A. Prohl, *Convergent finite element discretizations of the nonstationary incompressible magnetohydrodynamics system*, ESAIM Math. Model. Numer. Anal. 42 (2008), no. 6, 1065–1087. https://doi.org/10.1051/m2an:2008034.
[17] Z. Xiang, *On the Cauchy problem for the compressible Hall-magneto-hydrodynamics equations*, J. Evol. Equ. 17 (2017), 685–715.
[18] G. Yuksel and R. Ingram, *Numerical analysis of a finite element, Crank-Nicolson discretization for MHD flows at small magnetic Reynolds numbers*, Int. J. Numer. Anal. Model. 10 (2013), no. 1, 74–98.
[19] R. Hiptmair, L. Li, S. Mao, and W. Zheng, *A fully divergence-free finite element method for magnetohydrodynamic equations*, Math. Models Methods Appl. Sci. 28 (2018), no. 4, 659–695. https://doi.org/10.1142/S0218202518500173.
[20] J. Zhao, S. Mao, and W. Zheng, *Anisotropic adaptive finite element method for magnetohydrodynamic flow at high Hartmann numbers*, Appl. Math. Mech. (English Ed.) 37 (2016), no. 11, 1479–1500. https://doi.org/10.1007/s10483-016-2107-9.
[21] A. J. Chorin, *Numerical solution of the Navier-Stokes equations*, Math. Comput. 22 (1968), 745–762.
[22] R. Temam, *Sur l'approximation de la solution des équations de Navier-Stokes par la méthode des pas fractionnaires II*, Arch. Ration. Mech. Anal. 33 (1969), 377–385.
[23] J. B. Bell, P. Colella, and H. M. Glaz, *A second-order projection method for the incompressible Navier-Stokes equations*, J. Comput. Phys. 85 (1989), no. 2, 257–283. https://doi.org/10.1016/0021-9991(89)90151-4.
[24] P. M. Gresho, *On the theory of semi-implicit projection methods for viscous incompressible flow and its implementation via a finite element method that also introduces a nearly consistent mass matrix. I. Theory*, Int. J. Numer. Methods Fluids 11 (1990), no. 5, 587–620. [Computational methods in flow analysis (Okayama, 1988)]. https://doi.org/10.1002/fld.1650110509.
[25] J. Kim and P. Moin, *Application of a fractional-step method to incompressible Navier-Stokes equations*, J. Comput. Phys. 59 (1985), no. 2, 308–323. https://doi.org/10.1016/0021-9991(85)90148-2.
[26] R. Rannacher, "On Chorin's projection method for the incompressible Navier-Stokes equations," *The Navier-Stokes equations II—Theory and numerical methods*, Lecture Notes in Mathematics, Vol 1530, Springer, Berlin, 1992, pp. 167–183.
[27] E. Weinan and J.-G. Liu, *Projection method. I. Convergence and numerical boundary layers*, SIAM J. Numer. Anal. 32 (1995), no. 4, 1017–1057. https://doi.org/10.1137/0732047.
[28] J. Shen, *Remarks on the pressure error estimates for the projection methods*, Numer. Math. 67 (1994), no. 4, 513–520. https://doi.org/10.1007/s002110050042.
[29] J. L. Guermond and J. Shen, *On the error estimates for the rotational pressure-correction projection methods*, Math. Comput. 73 (2004), no. 248, 1719–1737. https://doi.org/10.1090/S0025-5718-03-01621-1.
[30] J. Shen, *On error estimates of projection methods for Navier-Stokes equations: First-order schemes*, SIAM J. Numer. Anal. 29 (1992), no. 1, 57–77.
[31] J. Shen, *On error estimates of some higher order projection and penalty-projection methods for Navier-Stokes equations*, Numer. Math. 62 (1992), no. 1, 49–73. https://doi.org/10.1007/BF01396220.
[32] J. Shen, *On error estimates of the projection methods for the Navier-Stokes equations: Second-order schemes*, Math. Comput. 65 (1996), no. 215, 1039–1065.

[33] A. J. Chorin, *On the convergence of discrete approximations to the Navier-Stokes equations*, Math. Comput. 23 (1969), 341–353. https://doi.org/10.2307/2004428.

[34] A. Prohl, *Projection and quasi-compressibility methods for solving the incompressible Navier-Stokes equations*, Advances in Numerical Mathematics, B. G. Teubner, Stuttgart, 1997.

[35] A. Prohl, *On pressure approximation via projection methods for nonstationary incompressible Navier-Stokes equations*, SIAM J. Numer. Anal. 47 (2008), no. 1, 158–180. https://doi.org/10.1137/07069609X.

[36] J. L. Guermond, J. Shen, and X. Yang, *Error analysis of fully discrete velocity-correction methods for incompressible flows*, Math. Comput. 77 (2008), no. 263, 1387–1405. https://doi.org/10.1090/S0025-5718-08-02109-1.

[37] J. L. Guermond and L. Quartapelle, *On the approximation of the unsteady Navier-Stokes equations by finite element projection methods*, Numer. Math. 80 (1998), no. 2, 207–238. https://doi.org/10.1007/s002110050366.

[38] H. Choi and J. Shen, *Efficient splitting schemes for magneto-hydrodynamic equations*, Sci China Math 59 (2016), no. 8, 1495–1510. https://doi.org/10.1007/s11425-016-0280-5.

[39] R. An and Y. Li, *Error analysis of first-order projection method for time-dependent magnetohydrodynamics equations*, Appl. Numer. Math. 112 (2017), 167–181. https://doi.org/10.1016/j.apnum.2016.10.010.

[40] X. Yang, G. D. Zhang, and X. He, *Convergence analysis of an unconditionally energy stable projection scheme for magneto-hydrodynamic equations*, Appl. Numer. Math. 136 (2019), 235–256. https://doi.org/10.1016/j.apnum.2018.10.013.

[41] M. Costabel and M. Dauge, *Singularities of Maxwell's equations on polyhedral domains*, Pitman Research Notes in Mathematics Series, Vol 379, Longman, Stuttgart, 1998, 69–76.

[42] M. Costabel and M. Dauge, *Singularities of electromagnetic fields in polyhedral domains*, Arch. Ration. Mech. Anal. 151 (2000), no. 3, 221–276. https://doi.org/10.1007/s002050050197.

[43] M. Costabel and M. Dauge, *Weighted regularization of Maxwell equations in polyhedral domains. A rehabilitation of nodal finite elements*, Numer. Math. 93 (2002), no. 2, 239–277. https://doi.org/10.1007/s002110100388.

[44] M. Dauge, *Singularities of corner problems and problems of corner singularities*, ESAIM Proceedings of the Society of Applied and Industrial Mathematics, Vol 6, Society for Industrial and Applied Mathematics, Paris, 1999, 19–40.

[45] D. Schötzau, *Mixed finite element methods for stationary incompressible magneto-hydrodynamics*, Numer. Math. 96 (2004), no. 4, 771–800. https://doi.org/10.1007/s00211-003-0487-4.

[46] H. Gao and W. Qiu, *A semi-implicit energy conserving finite element method for the dynamical incompressible magnetohydrodynamics equations*, Comput. Methods Appl. Mech. Eng. 346 (2019), 982–1001.

[47] L. Baňas and A. Prohl, *Convergent finite element discretization of the multi-fluid nonstationary incompressible magnetohydrodynamics equations*, Math. Comput. 79 (2010), no. 272, 1957–1999. https://doi.org/10.1090/S0025-5718-10-02341-0.

[48] C. Greif, D. Li, D. Schötzau, and X. Wei, *A mixed finite element method with exactly divergence-free velocities for incompressible magnetohydrodynamics*, Comput. Methods Appl. Mech. Eng. 199 (2010), no. 45–48, 2840–2855. https://doi.org/10.1016/j.cma.2010.05.007.

[49] P. Houston, D. Schötzau, and X. Wei, *A mixed DG method for linearized incompressible magnetohydrodynamics*, J. Sci. Comput. 40 (2009), no. 1–3, 281–314. https://doi.org/10.1007/s10915-008-9265-x.

[50] P. Monk, *Finite element methods for Maxwell's equations*, Numerical Mathematics and Scientific Computation, Oxford University Press, New York, 2003.

[51] D. Boffi, F. Brezzi, and M. Fortin, *Mixed finite element methods and applications*, Springer Series in Computational Mathematics, Vol 44, Springer, Heidelberg, 2013.

[52] V. Girault and P. A. Raviart, "Theory and algorithms," *Finite element methods for Navier-Stokes equations*, Springer Series in Computational Mathematics, Vol 5, Springer-Verlag, Berlin, 1986.

[53] J. C. Nédélec, *Mixed finite elements in* $\boldsymbol{R}^3$, Numer. Math. 35 (1980), no. 3, 315–341.

[54] R. Hiptmair, *Finite elements in computational electromagnetism*, Acta Numer. 11 (2002), 237–339. https://doi.org/10.1017/S0962492902000041.

[55] P. G. Ciarlet, *The finite element method for elliptic problems*, Studies in Mathematics and its Applications, Vol 4, North-Holland Publishing Co., Amsterdam, 1978.

[56] F. Brezzi and M. Fortin, *Mixed and hybrid finite element methods*, Springer Series in Computational Mathematics, Vol 15, Springer-Verlag, New York, 1991.

[57] J. L. Guermond, *Some implementations of projection methods for Navier-Stokes equations*, RAIRO Modél. Math. Anal. Numér. 30 (1996), no. 5, 637–667. https://doi.org/10.1051/m2an/1996300506371.

[58] J. Shen and X. Yang, *Error estimates for finite element approximations of consistent splitting schemes for incompressible flows*, Discrete Contin. Dyn. Syst. Ser. B 8 (2007), no. 3, 663–676. https://doi.org/10.3934/dcdsb.2007.8.663.

[59] J. G. Heywood and R. Rannacher, *Finite-element approximation of the nonstationary Navier-Stokes problem. IV. Error analysis for second-order time discretization*, SIAM J. Numer. Anal. 27 (1990), no. 2, 353–384.

[60] D. Boffi, *Fortin operator and discrete compactness for edge elements*, Numer. Math. 87 (2000), no. 2, 229–246.

[61] B. Li and W. Sun, *Error analysis of linearized semi-implicit Galerkin finite element methods for nonlinear parabolic equations*, Int. J. Numer. Anal. Model. 10 (2013), no. 3, 622–633.

[62] D. Shi, J. Wang, and F. Yan, *Unconditional superconvergence analysis for nonlinear parabolic equation with EQ_1^{rot} nonconforming finite element*, J. Sci. Comput. 70 (2017), no. 1, 85–111. https://doi.org/10.1007/s10915-016-0243-4.

[63] D. Shi and J. Wang, *Unconditional superconvergence analysis of conforming finite element for nonlinear parabolic equation*, Appl. Math. Comput. 294 (2017), 216–226. https://doi.org/10.1016/j.amc.2016.08.024.

[64] J. Wang, *Superconvergence analysis for nonlinear reaction-diffusion equation with BDF-FEM*, Math. Meth. Appl. Sci. 43 (2020), 4732–4743.

[65] L. Zhang, T. Cui, and H. Liu, *A set of symmetric quadrature rules on triangles and tetrahedra*, J. Comput. Math. 27 (2009), no. 1, 89–96.

[66] L. B. Zhang, *A parallel algorithm for adaptive local refinement of tetrahedral meshes using bisection*, Numer. Math. Theory Methods Appl. 2 (2009), no. 1, 65–89.

How to cite this article: Q. Ding, X. He, X. Long, and S. Mao, *Error analysis of a fully discrete projection method for magnetohydrodynamic system*, Numer. Methods Partial Differ. Eq. **39** (2023), 1449–1477. https://doi.org/10.1002/num.22941